Aalto University
School of Chemical
Technology

School of Chemical Technology
Degree Programme of Chemical Technology

Iiro Kiiski

DEVELOPMENT OF IMMOBILIZED ENZYME MICROREACTORS FOR CYTOCHROME P450 MEDIATED DRUG METABOLISM

Master's thesis for the degree of Master of Science in Technology submitted for inspection, Espoo, 4 August, 2016.

Supervisor Professor Alexander Frey

Instructor PhD (pharm.) Tiina Sikanen

Aalto University
School of Chemical
Technology

Aalto University, P.O. BOX 11000, 00076 AALTO
www.aalto.fi

Abstract of master's thesis

Author Iiro Kiiski

Title of thesis Development of immobilized enzyme microreactors for studying cytochrome P450 mediated drug metabolism

Department Biotechnology and Chemical Technology

Professorship Molecular biotechnology **Code of professorship** KE-70

Thesis supervisor Alexander Frey

Thesis advisor(s) / Thesis examiner(s) Tiina Sikanen

Date 4.8.2016 **Number of pages** 83+1 **Language** english

Abstract

The cytochrome P450 (CYP) enzyme family is responsible for eliminating exogenous chemicals from the human body. As most drugs are metabolized by the same small number of CYP isoenzymes, the risk of drug-drug interactions grows as the use of drugs increases. Consequently, it is important to study the metabolic pathways of a new drug candidate as early in the development pipeline as possible to be able to either modify the molecule or abandon the candidate before continuing to the cost-intensive clinical stage.

The general aim of this thesis was to develop new immobilization methods for cytochrome P450 enzymes with a view to implementation of immobilized enzyme microreactors for pharmaceutical applications. Two main approaches for immobilizing CYP-containing human liver microsomes (HLM) were studied: the immobilization of HLM on commercial streptavidin-coated magnetic particles and the immobilization of HLM on in-house fabricated thiol-ene based microfluidic chips. On the basis of literature search, a novel immobilization method utilizing biotin-labelled fusogenic liposomes (FL) was developed.

When immobilizing HLM on magnetic particles, the use of FL conferred a 3-fold increase in enzyme activity compared to a previously published method based on physical adsorption on the bead surface. The K_m value of the immobilized HLM was determined, and was comparable to the K_m of the soluble HLM (2.5 ± 0.49 μM and 0.5-2 μM, respectively), which is essential for the prospective applications in metabolic studies. Enzyme stability remains an issue, as the activity of the immobilized enzyme quickly decreased with consecutive incubations, probably due to both thermal inactivation and leaching.

Three different methods for HLM immobilization on thiol-ene micropillar chips were studied. HLM were solubilized on a chip surface functionalized with lipid bilayers and HLM labeled with biotin using FL was bound on streptavidin-functionalized chip surface. For comparison, HLM was also immobilized on chip surface by physical adsorption. The highest initial activities could be achieved by adsorption, but the activity also decreased very rapidly. With the other two methods, initial reactor activities were lower, but the decline of enzyme activity could be slowed down. However, the enzyme activity of all reactors faded within 2 hours.

In the future, practical applications based on the developed immobilization approaches could be developed for *in vitro* studies of human drug metabolism. Another valid application for these reactors is the *in situ* preparation of analytical standards of CYP metabolites.

Keywords cytochrome P450, drug metabolism, microfluidics, immobilization

Aalto University
School of Chemical
Technology

Aalto University, P.O. BOX 11000, 00076 AALTO
www.aalto.fi

Abstract of master's thesis

Tekijä Iiro Kiiski

Työn nimi Immobilisoitujen entsyymimikroreaktorien kehittäminen sytokromi P450 -välitteisen lääkeainemetabolian tutkimiseen

Laitos Biotekniikan ja kemian tekniikan laitos

Professuuri molekyylibioteknologia **Professuurikoodi** KE-70

Työn valvoja Alexander Frey

Työn ohjaaja(t)/Työn tarkastaja(t) Tiina Sikanen

Päivämäärä 4.8.2016 **Sivumäärä** 83+1 **Kieli** englanti

Tiivistelmä

Sytokromi P450 (CYP) entsyymiperhe vastaa vierasaineiden poistamisesta ihmiskehosta. Koska useimpien lääkeaineiden metaboliaa katalysoivat samat CYP-isoentsyymit, lääkeaineinteraktioiden riski kasvaa, kun lääkkeiden käyttö yhteiskunnassa lisääntyy. Uusien lääkeaineiden metaboliareittejä onkin tärkeää kartoittaa jo varhaisessa vaiheessa lääkekehitystä, jotta molekyyliä voidaan tarvittaessa muokata tai kehityslinja hylätä kokonaan ennen kallista kliinistä vaihetta.

Tämän työn tavoitteena oli kehittää uusia immobilisointimenetelmiä CYP-entsyymeille farmaseuttisia sovelluksia varten. Työssä tutkittiin kahta menetelmää CYP-entsyymejä sisältävien ihmisen maksamikrosomien (human liver microsomes, HLM) immobilisointiin. Entsyymejä immobilisoitiin sekä kaupallisten, streptavidiinipäällysteisten magneettipartikkeleiden pintaan että itse valmistettujen tioleenipohjaisten mikrosirujen pintaan. Tarkoitukseen kehitettiin kirjallisuushaun perusteella uusi, biotiinileimattuja fusogeenisiä liposomeja hyödyntävä immobilisointimenetelmä.

Fusogeenisten liposomien hyödyntäminen nosti magneettipartikkelien pintaan immobilisoitujen entsyymien entsyymiaktiivisuutta kolminkertaisesti verrattuna aikaisemmin raportoituun adsorptiopohjaiseen menetelmään. Immobilisoidulle HLM:lle määritetty K_m-arvo (2.5 ± 0.49 μM) vastasi hyvin kirjallisuudessa liukoiselle HLM:lle raportoitua arvoa (0.5-2 μM), mikä on oleellista mahdollisten tulevien sovellusten kannalta. Immobilisoidun entsyymin aktiivisuus kuitenkin laski nopeasti perättäisten inkubointien seurauksena, mikä johtui todennäköisesti sekä entsyymin huuhtoutumisesta että lämmön aikaansaamasta inaktivaatiosta.

Tioleenipohjaisten mikrosirujen pintaan mikrosomeja immobilisoitiin kolmella menetelmällä. Mikrosomeja liuotettiin lipidi-kaksoiskerroksella funktionalisoidun kanavan pintaan ja biotiinilla leimattuja mikrosomeja immobilisoitiin streptavidiinilla funktionalisoidun sirun pintaan. Verrokkisirussa HLM immobilisoitiin sirun pintaan fysikaalisen adsorption avulla. Suurin alkuaktiivisuus saavutettiin adsorptiolla, mutta entsyymiaktiivisuus myös laski nopeasti. Kahta muuta menetelmää hyödyntämällä alkuaktiivisuudet olivat matalampia, mutta aktiivisuus myös tippui hitaammin. Kaikkien reaktorityyppien aktiivisuus hävisi kahden tunnin sisällä reaktion aloittamisesta.

Tulevaisuudessa työssä kehitettyjä immobilisointimenetelmiä voidaan käyttää pohjana suunniteltaessa käytännön sovelluksia ihmisen vierasainemetabolian tutkimiseen. Toinen mahdollinen sovelluskohde kehitetyille entsyymireaktoreille on analyyttisten metaboliittistandardien tuottaminen.

Avainsanat sytokromi P450, lääkeainemetabolia, mikrofluidistiikka, immobilisointi

Contents

Preface

This thesis was carried out within the CUMTAS (Customized Micro Total Analysis Systems to Study Human Phase I Metabolism) project in the Division of Pharmaceutical Chemistry, Faculty of Pharmacy, University of Helsinki from January to May 2016. First and foremost I would like to thank my instructor Ph.D. (Pharm.) Tiina Sikanen for allowing me to work in this magnificent project under her guidance. I couldn't have wished for a more competent and compassionate mentor. I would also like to thank my supervisor, Professor Alexander Frey for his invaluable advice during the making of this thesis. I am also thankful for the amazing bunch of workmates I had at the chemical microsystems group. It was a pleasure working with you.

I devote my deepest gratitude to my parents, without whose love and support I could not have come this far. Heartfelt thanks are also due to all my friends that have supported me and helped me to take my mind off of all things science. Last but most definitely not least: Thank you Reetta for your continuous understanding and support.

Helsinki, 2.8.2016

Iiro Kiiski

Abbreviations and symbols

CLEA	cross-linked enzyme aggregates
CLEC	cross-linked enzyme crystals
CYP	cytochrome P450
DLS	dynamic light scattering
DMF	digital microfluidics
DMSO	dimethyl sulfoxide
DOPE	1,2-dioleoyl-sn-glycero-3-phosphoethanolamine
DOTAP	1,2-dioleoyl-3-trimethylammonium-propane
EDC	(N-(3-Dimethylaminopropyl)-N′-ethylcarbodiimide hydrochloride
FDA	U.S. Food and Drug Administration
FL	fusogenic liposomes
HLM	human liver microsomes
HPLC	high-performance liquid chromatography
IMER	immobilized enzyme microreactor
LC	liquid chromatography
LIF	laser-induced fluorescence
LUV	large unilamellar vesicles
MES	2-(N-morpholino)ethanesulfonic acid
MLV	multilamellar vesicles
μTAS	micro total analysis systems
MS	mass spectrometer
NADPH	nicotinamide adenine dinucleotide phosphate
NADPH-CPR	NADPH cytochrome P450 reductase
NHS	(N-hydroxysuccinimide)
PBS	phosphate buffered saline

PDI	polydispersity index
PDMS	polydimethylsiloxane
SEM	scanning electron microscope
SPE	solid phase extraction
SU-8	trademark of an epoxy polymer (glycidyl ether of bisphenol A)
SUV	small unilamellar vesicles
T_m	lipid phase transition temperature
UV	ultraviolet

1 Introduction

The cytochrome P450 (CYP) enzyme family is responsible for eliminating exogenous chemicals from the human body. Because most drugs are metabolized by the same small number of CYP isoenzymes in humans, the risk of drug-drug interactions is bound to increase as the use of new multiple-drug therapies and the use of drugs as a whole increase. Therefore, it is of paramount interest to study the metabolic pathways of new drug candidates as early in the development pipeline as possible to be able to either modify the molecule or to abandon the candidate before the cost-intensive clinical stage.

The degradation processes of pharmaceuticals in the environment are presently poorly understood. The lack of commercial drug metabolite standards is hampering the efforts to evaluate the full environmental load of a given pharmaceutical (Celiz *et al.* 2009). Immobilized CYP microreactors (IMERs) can also be utilized in *in situ* analyte preparation.

The research area of micro total analysis systems (μTAS), also known as “lab on a chip” was established some 25 years ago, and has grown and developed rapidly ever since. The μTAS technology allows the integration of various analytical steps, such as sample pretreatment, separation and detection, on a single chip. Integration and miniaturization bring along many advantages. Only minute sample volumes are needed for each analysis. Enhanced mass and heat transfer enabled by shorter diffusion distances mean that μTAS systems run with higher throughput compared to their bigger counterparts. With smaller volumes, the amount of waste and the use of costly chemicals are also reduced. (Culbertson *et al.* 2014; Kovarik *et al.* 2012; Vilkner *et al.* 2004). The prospect of increased throughput and convenient tailoring by means of miniaturization and integration have raised special interest in the fields of biological and biomedical analysis, from where a major part of novel microfluidic applications are stemming (Culbertson *et al.* 2014; Kovarik *et al.* 2012). As a concrete sign of this, published items using both of the keywords “microfluidics” and “*in vitro*”, has grown steadily over the last ten years according to the ISI Web of Knowledge (Figure 1).

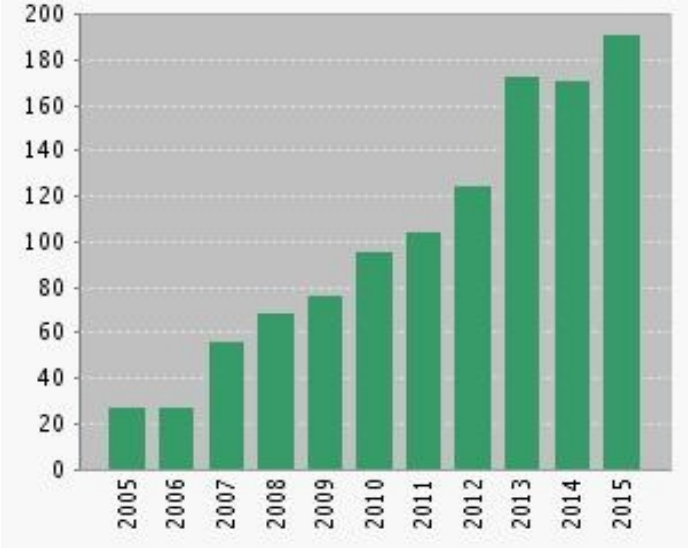

Figure 1. Number of publications per year using the keywords "microfluidics" and *"in vitro*" from 2005-2015 (ISI Web of knowledge, https://webofknowledge.com).

Immobilization of enzymes offers many advantages over using soluble enzymes. By immobilization, the enzyme is compartmentalized in a confined space and easily separated from the product, which facilitates further handling of the product. Immobilization also allows for the reuse and recovery of costly enzymes, which may often be a requisite for economic viability of industrial enzyme-catalyzed processes (Tischer & Wedekind 1999; Sheldon 2007; Mohamad *et al.* 2015). An additional benefit is the often enhanced stability towards denaturation both under storage and in operational conditions (Cabral & Kennedy 1993).

Many challenges still remain in the field of microfluidic metabolic studies. The detection technology in microfluidics is still to a large extent based on the conventional, macro-scale instrumentation, which sets certain limitations to detection sensitivity (Sikanen 2013). The stability of immobilized CYPs is often very poor, which undermines the effective reuse of CYP reactors. This thesis attempts to address these issues by the development of novel immobilization methods for CYP enzymes.

The aim of this study is to develop new immobilization methods for cytochrome P450 enzymes with a view to implementation of immobilized enzyme microreactors for pharmaceutical applications. Two main approaches for HLM immobilization are studied: The immobilization of HLM on commercial streptavidin-coated magnetic particles and the immobilization of HLM on in-house

fabricated thiol-ene-based microfluidic pillar channels featuring a dense micropillar array. In both cases the feasibility of a novel immobilization method utilizing fusogenic biotin-labelled liposomes is assessed in comparison to nonspecific adsorption on magnetic particles or on the channel surface.

2 Literature review

2.1 Human drug metabolism

2.1.1 Overview

Most drugs of clinical use have lipophilic properties, because otherwise they would not be absorbed in sufficient amounts. Lipophilic substances cannot be efficiently excreted from the body, and so the continuous uptake of such chemicals would lead to their accumulation in the body, unless we had an effective elimination mechanism such as drug metabolizing enzymes. The main function of drug metabolism is to increase the hydrophilicity of foreign substances to facilitate their elimination through the kidneys or the intestine (Zanger 2012).

The metabolic pathway of a drug is usually divided into phase I and phase II reactions. Phase I reactions comprise of functionalization reactions mostly catalyzed by enzymes belonging to the cytochrome P450 (CYP) family. Phase I reactions are usually a preparatory step followed by conjugation of the newly created group to a hydrophilic moiety (e.g. glutathione, glucuronic acid) in phase II reactions catalyzed by different transferase enzymes. However, it should be noted that many drugs are cleared only via phase I or phase II reactions, or even by pathways in the reverse order (Zanger 2012).

2.1.2 Drug-drug interactions

Although phase II reactions also play a significant role in human drug metabolism, CYP enzymes are the major constituents of metabolic pathways. According to Guencerich (2008), about 75% of drugs are metabolized primarily by CYPs. The nomenclature of CYP enzymes employs a three-tiered classification based on the evolution of the superfamily. The family (40% homology in amino acid sequence), subfamily (55% homology) and individual gene are indicated by an Arabic number, capital letter and another Arabic number, respectively (Nebert *et al.* 1991).

The isoenzymes responsible for the majority of hepatic drug metabolism are CYP3A4, CYP2D6 and CYP2C9 (Shimada *et al.* 1994). The fact that the majority of drugs are metabolized by the same CYP isoenzymes can result in metabolic interactions between co-administered drugs. The alteration in metabolic rates can lead to clinically significant changes in drug plasma concentrations. The proportion of metabolic reactions catalyzed by CYP enzymes and the relative proportions of different CYP isoenzymes are illustrated in Figure 2.

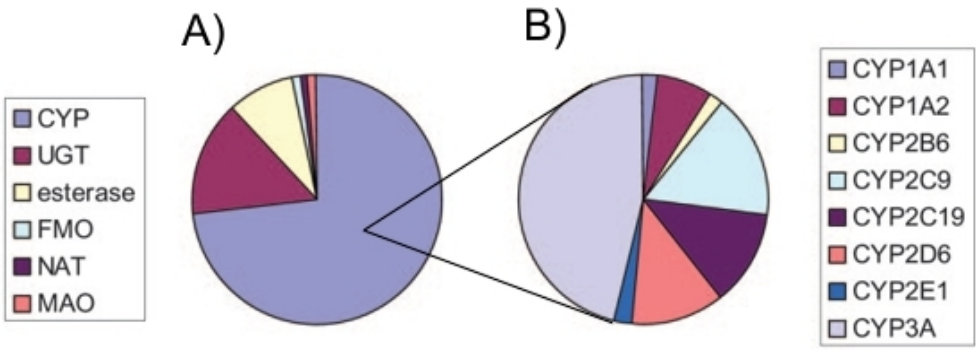

Figure 2. A) Contributions of different enzymes to the metabolism of 200 most prescribed drug in the US in 2002. UGT: Uridine 5'-diphospho-glucuronosyltransferase, FMO: flavin-containing monoxygenase, NAT: N-acetyltransferase and MAO: monoamine oxidase. B) Metabolism reactions of drugs catalyzed by individual CYP enzymes. (Williams *et al.* 2004*)*

Clinically significant drug-drug interactions occur when 2 or more drugs are metabolized by the same isoenzyme and when the reaction catalyzed by a single isoenzyme is the major or only elimination pathway of at least one of the drugs. Two drugs can interfere with each other's elimination via CYP inhibition or CYP induction. CYP inhibition is caused by direct interaction of a drug with a given CYP isoenzyme and can be either reversible or irreversible. Irreversible, or mechanism-based CYP inhibition involves permanent inactivation of CYP enzymes. Reversible inhibition can be further classified as competitive, non-competitive or uncompetitive depending on whether the inhibitor binds directly to the active site (competitive) or elsewhere (non-competitive or uncompetitive). Some human CYP isoenzymes are also inducible. CYP induction is a slow regulatory process that can lower the plasma concentrations of a drug and thus compromise its efficacy. Induction is mainly caused by an increase in gene

transcription, but can also be the result of a decrease in CYP protein degradation. (Lin & Lu 1998; Tanaka 1998; Fowler & Zhang 2008).

In competitive inhibition, both the substrate and the inhibitor bind to the active site of the free enzyme, and binding of the inhibitor will consequently block the substrate from binding. Competitive inhibition is usually the mode of interaction for two drugs metabolized by the same CYP isoenzyme. In noncompetitive inhibition, the inhibitor binds to another site on the enzyme and has no effect on substrate binding, but the enzyme-substrate complex is unproductive in the presence of the inhibitor. In un-competitive inhibition, the inhibitor binds only to the enzyme-substrate complex, rendering it unproductive (Lin & Lu 1998; Fowler & Zhang 2008). The effects of all modes of inhibition on the Michaelis-Menten kinetics parameter values are summarized in Table 1 with equations describing the percentage of inhibition with given inhibitor and substrate concentrations.

Table 1. Kinetic characteristics of reversible inhibition models. PI = percentage of inhibition, [I] = inhibitor concentration, [S] = substrate concentration, K_i = inhibition constant, K_m = Michaelis-Menten constant.

Inhibition model	K_m	V_{max}	Percentage of inhibition
Competitive	increases	unchanged	$PI = \frac{\frac{[I]}{K_i}}{1 + \frac{[I]}{K_i} + \frac{[S]}{K_M}}$
Non-competitive	no effect	decreases	$PI = \frac{\frac{[I]}{K_i}}{1 + \frac{[I]}{K_i}}$
Uncompetitive	decreases	decreases	$PI = \frac{\frac{[I]}{K_i}}{1 + \frac{[I]}{K_i} + \frac{K_M}{[S]}}$

As can be seen from the equations in Table 1, the inhibitory effect of an inhibitor is dictated by its binding affinity to the active site of an enzyme, which is denoted by K_i. In the case of competitive inhibition, as in the case of two drugs metabolized through the same isoenzyme, inhibition is intelligibly also affected by the K_m of the substrate. In light of this, the essential goal of metabolism studies is

the prediction of *in vivo* kinetic parameters from *in vitro* data. When the kinetic properties of a particular drug or inhibitor are characterized, the information can be used to predict the enzymes involved in metabolism and/or inhibition at physiologically relevant concentrations (Korzewka 2008).

The standard approach to screening potential drug interactions is to determine the effect of a new substance on *in vitro* probe reactions. The probe reactions utilize compounds that are highly specific substrates for an individual isoenzyme and can be used to monitor the activity of that particular metabolic pathway (Korzewka 2008; Yuan *et al.* 2002). A list of recommended probe substrates for each CYP isoenzyme released by the United States Food and Drug Administration (FDA) can be found in Appendix 1. Coumarin 7-hydroxylation, the probe reaction used in this study, is a reaction catalyzed specifically by the CYP2A6 isoenzyme.

2.1.3 Cytochrome P450s

Cytochrome P450 isoenzymes are heme-containing proteins deriving their name from a characteristic spectral peak at 450 nm, owing to the binding of carbon monoxide to the ferrous heme iron. The catalytic activity of CYP enzymes involves binding and splitting molecular oxygen to its constituent atoms, inserting one of the oxygen atoms into a substrate bound by the CYP active site and reducing the other oxygen atom to water. The reduction of molecular oxygen requires a source of free electrons, which in the case of CYP reactions is usually nicotinamide adenine dinucleotide phosphate (NADPH) (Munro *et al.* 2013; Guengerich 2012). CYP enzymes can be categorized as monooxygenases catalyzing the generalized reaction:

$$NADPH + H^+ + R - H + O_2 \rightarrow NADP^+ + H_2O + R - OH \quad (1)$$

where RH is the substrate and ROH is the hydroxylated product. The classical reaction catalyzed by CYPs is indeed the hydroxylation of organic substrates. However, CYP enzymes are immensely versatile enzymes capable of catalyzing a myriad of different chemical transformations, such as O- and N-dealkylation (Munro *et al.* 2013).

The supply of electrons from NADPH is facilitated by a redox partner protein called NADPH cytochrome P450 reductase (NADPH-CPR) (Paine *et al.* 2005; Munro *et al.* 2013). In recent times, it has become evident that other proteins, such as cytochrome b_5 may also be involved in the complex redox chains of CYP reactions (Im & Waskell 2011; Munro *et al.* 2007). *In vivo*, all the different components are embedded in the cell membrane primarily in the endoplasmic reticulum of hepatocytes. This is facilitated by an N-terminal hydrophobic peptide sequence that anchors the proteins into the membrane (Munro *et al.* 2007). The presence of lipid bilayers is integral to CYP function by ensuring correct conformational arrangement. Lipid membranes also facilitate the interactions between CYPs and its redox partners by placing them close together on the same membrane (Imaoka *et al.* 1992).

A drug that reversibly binds to a CYP enzyme displays hyperbolic saturation kinetics. Under steady-state conditions, the velocity of a simple CYP-catalyzed metabolic reaction can be described by the Michaelis-Menten equation (Equation 2):

$$v = \frac{V_{max}[S]}{K_m + [S]} \qquad (2)$$

where v is the reaction velocity and K_m and V_{max} are enzyme-substrate pair specific constants describing the reaction kinetics. V_{max} is the maximal reaction velocity achieved at saturating substrate concentrations, and K_m is the substrate concentration where the reaction velocity is half of V_{max} (Copeland 2000; Korzewka 2008). It should be noted that many examples of non Michaelis-Menten kinetics have also been observed for CYP mediated reactions (Fowler & Zhang 2008).

2.1.4 Cytochrome P450 *in vitro* models

Several *in vitro* models have been developed for studying hepatic drug metabolism. These include supersomes (baculovirus-expressed CYP), liver microsomal fractions, transgenic cell lines, primary hepatocytes, liver slices and perfused livers (Brandon *et al.* 2003). As for the purposes of this thesis, it suffices

to discuss in detail three of these models that aptly represent the whole variety of all available models. The discussed models are human liver microsomes (HLM), human recombinant enzymes and hepatocytes.

HLM is the most popular and widely used model used in metabolic profiling and drug interaction studies (Fasinu *et al.* 2012). HLM consist of vesicles of hepatocyte endoplasmic reticulum that are prepared by using differential centrifugation. All CYP isoenzymes (as well as NADPH-CPR) can be found in a microsomal reparation. HLM can be prepared from various sources, such as fresh human liver and liver cell lines. The variance in HLM activity between individuals can be tackled by pooling a large bank of liver tissues together. HLM offer a relatively affordable, very established method for studying drug metabolism. As studies conducted using HLM are also considered to most closely simulate the *in vivo* situation, they are the industry standard for drug interaction studies (Fowler & Zhang 2008). The use of HLM does have some drawbacks. While the presence of all isoenzymes may be useful when mimicking *in vivo* conditions, it is a disadvantage when determining which enzymes are involved in the metabolism of a particular drug. Because of the broad substrate selectivity of CYP enzymes, most reactions can be catalyzed by more than one enzyme (Korzewka 2008). Also, CYP are enriched in the microsomal fraction, which results in higher metabolic rates compared to the *in vivo* situation. This means that HLM assays cannot be used for direct quantitative estimations. It should also be noted that because HLM are not composed of intact cells and therefore lack active gene transcription, they cannot be used to study enzyme induction by drugs (Brandon *et al.* 2003; Fasinu *et al.* 2012).

The most popular way of producing recombinant CYP enzymes is the baculovirus-based expression in insect cells. As insect cells lack endogenous CYP activity, it is possible to prepare microsomal vesicles containing recombinant human CYP enzymes. These microsomes are marketed by the name supersome (Gentest) or baculosome (Thermo Fischer). Because only the expressed human CYP isoforms are present, supersomes allow the assessment of individual isoenzymes and their ability to metabolize the drug in question. However, recombinant enzymes cannot be used to predict to which extent a given isoenzyme metabolizes a drug *in vivo*, as no alternative pathways are present.

(Fasinu *et al.* 2012; Brandon *et al.* 2003). With the use of protein engineering, it is also possible to manufacture soluble human CYP enzymes that need no lipid membrane by truncating the hydrophobic membrane N-terminus sequence (Kumar 2010; Yun *et al.* 2006). This does not however remove the need for the auxiliary proteins or an electron source.

Isolated primary hepatocytes are a popular *in vitro* model owing to their strong resemblance of *in vivo* conditions. Hepatocytes are isolated directly from human liver. Advantages of hepatocytes include preservation of *in vivo* levels of different CYP enzymes and the possibility of studying inductive processes, as hepatocytes are intact cells with active gene expression (Fasinu *et al.* 2012; Brandon *et al.* 2003). Hepatocytes can be cryopreserved in liquid nitrogen for extended periods (McGinnity *et al.* 2004) but otherwise have a very limited viability from a few hours in solution to a few weeks with specialized culture techniques (Fasinu *et al.* 2012; Brandon *et al.* 2013). Commercial hepatocytes are presently available, but they are considerably more expensive compared to e.g. HLM.

2.2 Enzyme immobilization

Enzyme immobilization techniques can be generally divided into three main groups. Enzymes can be (i) bound to an inert support material via physical or chemical interactions, (ii) entrapped inside a porous matrix or (iii) cross-linked together to from enzyme aggregates or crystals. The classification of different enzyme immobilization methods is illustrated in Figure 3.

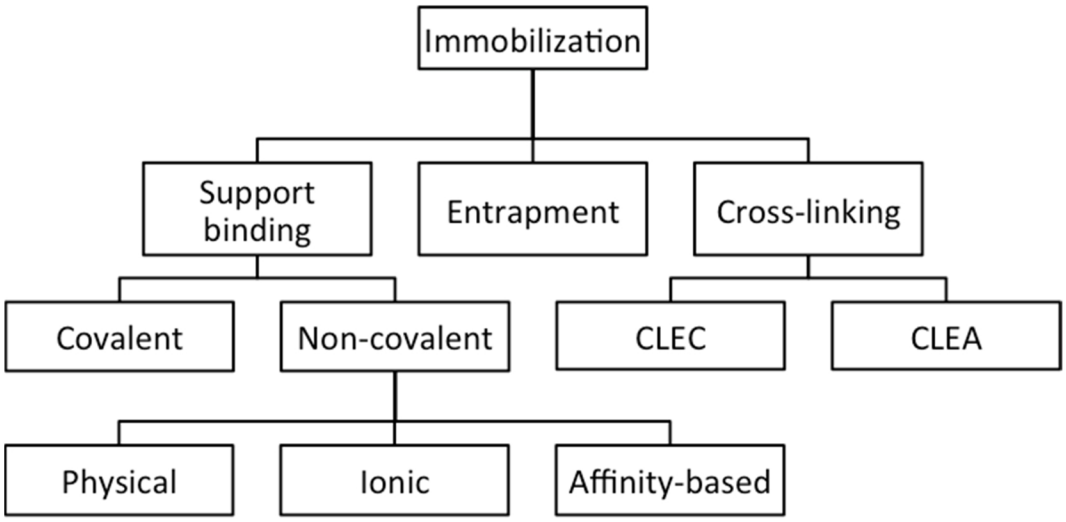

Figure 3. Classification of enzyme immobilization methods.

2.2.1 Support binding

Enzymes can be bound to a support material *via* both covalent and non-covalent bonds. The non-covalent binding methods based on the adsorption of enzymes on the support surface can be further divided into physical (hydrophobic and van der Waals interactions), ionic (electrostatic interactions) and affinity-based (e.g. biotin-avidin) methods (Wong *et al.* 2009; Sheldon 2007).

Owing to the low energies associated with non-covalent bonds, enzymes are easily washed away from the carrier surface, especially in more demanding conditions, such as elevated temperatures (Wong *et al.* 2009; Sheldon 2007). On the other hand, weak interactions do not usually alter the tertiary structure of the enzymes which helps the enzymes to retain their activity (Jesionowski *et al.* 2014).

The use of covalent bonds allows for a more stable anchorage between the enzyme and the carrier surface. The traditional noncovalent binding chemistries rely on naturally present functional groups (e.g. NH_2 and COOH) meaning that there is no need for prior enzyme modification. As there is no effective control over where the covalent bond will be formed, conventional covalent immobilization methods will generate a heterogeneous population of enzyme due to the random orientation of the immobilized biomolecules. If charged amino acid

residues are used for immobilization, the alteration of protein surface charge will also likely affect enzyme activity due to detrimental changes in protein folding (Wong *et al.* 2009).

2.2.2 Entrapment

In entrapment, enzymes are immobilized by physically trapping them inside a natural or synthetic polymer matrix. The polymer network is synthetized in the presence of the enzyme, and the enzyme is trapped inside the matrix due to physical restraints caused by the polymer pore size. With entrapment, high enzyme concentrations per volume can be achieved with relatively mild immobilization conditions (Kim & Herr 2013; Sumitra *et al.* 2012). As the method is not based on e.g. the surface chemistry of the enzyme, it is readily applied to a variety of different enzymes. The main disadvantages of entrapment are leaching of entrapped enzyme and impaired diffusion (Sheldon 2007). Impaired diffusion is due to the steric constraints caused by the polymer matrix that affect substrate diffusion to the active site of the enzyme. In these cases enzyme kinetics is usually limited by diffusion rates instead of the enzyme reaction rate itself.

Commonly used entrapment matrices include different kinds of sol-gels and hydrogels. Sol-gels are formed by drying colloidal solutions of metal oxides. Typical sol-gel precursors are silicon alkoxides (Sheldon & van Pelt 2013). Hydrogels are hydrophilic, cross-linked polymer chains. Compared to sol-gels, hydrogels are more biocompatible and no toxic reagents are needed in the polymerization process. Hydrogels are also usually transparent, which allows for the use of different imaging technologies. Commonly used hydrogel polymers include the synthetic poly(ethylene glycol) diacrylate and polyacrylamide and the natural polymers chitosan and agarose (Honiger *et al.* 1995).

2.2.3 Cross-linking

By cross-linking, carrierless macroparticles can be prepared from enzyme aggregates or crystals. The use of a carrier in methods described in sections 2.1.1 and 2.1.2 leads to ‘dilution’ of enzyme activity, as a large portion of the reactor volume is filled by non-catalytic material. The use of cross-linked,

carrierless enzymes enables highly concentrated enzyme activities without the need for an additional (often expensive) carrier (Sheldon & van Pelt 2013; Sheldon 2007).

Cross-linking techniques can be divided into two categories depending on the physical state of the enzyme before cross-linking. Cross-linked enzyme crystals (CLECs) are prepared by crystallizing the enzymes from an aqueous solution and cross linking the formed crystals by the addition of a bifunctional reagent, such as glutaraldehyde. The resulting cross-linked crystals are highly active and stable, and their particle size can be readily controlled. However, crystallizing proteins is a laborious procedure that requires enzyme of high purity. This drawback of CLECs can be avoided by the use of enzyme aggregates as the starting material for cross-linking. Enzyme aggregates can be easily prepared by the addition of salts or water miscible organic solvents to aqueous solutions of enzymes without affecting their tertiary structure. Subsequent cross-linking of these aggregates generates cross-linked enzyme aggregates (CLEAs). As protein precipitation is often used for purification, both purification and immobilization can be combined into a single unit operation that can be used, for example, to immobilize an enzyme directly from a crude fermentation broth (Sheldon & van Pelt 2013; Sheldon 2007).

2.2.4 Immobilization of cytochrome P450 enzymes

As discussed in section 2.1.3, CYPs constitute a complex enzymatic system. Reactions require both the CYP enzymes themselves as well as various redox partner enzymes. Also the cofactor NADPH and oxygen need to be supplied for the reactions to occur. All the enzyme components need to be embedded in a lipid bilayer to ensure catalytic activity. All these aspects place special demands on immobilization approaches of CYP enzymes. Moreover, when designing microfluidic applications for *in vitro* metabolic studies in particular, the system should accurately resemble *in vivo* conditions. For example, to draw relevant conclusions from *in vitro* studies, the immobilization of the enzyme should not affect the K_m values of the studied analytes, which places even further demands for the immobilization procedure. As HLM were used as a source for CYP

enzymes in this thesis, mainly approaches regarding the immobilization of HLM will be discussed in this section.

Different types of entrapment approaches are the typical immobilization methods used for human liver microsomes (Zguris *et al.* 2005; Sakai-Kato *et al.* 2005; Ma *et al.* 2009; Mao *et al.* 2012). A possible explanation for the preference of entrapment over other immobilization strategies is that it is best applicable for membrane-embedded protein structures. Entrapment in sol-gels or hydrogels does not affect the surface chemistry of the microsomes, as immobilization is based solely on physical constraints of the polymer network. It could also be argued that because the proteins in microsomes are embedded within the phospholipid membrane, the efficiency of covalent immobilization methods based on the chemistry of amino acids is diminished.

Membrane-bound CYP have also been immobilized on lipid bilayers on solid supports. This approach was studied also in this thesis on thiol-ene-based microreactors. Yoshihiro *et al.* (2007) immobilized microsomes containing rat CYP1A1 on the surface of micropatterned lipid bilayer membranes on glass substrates. This approach is similar to the entrapment strategies in the sense that it targets the whole microsomal vesicle, rather than the CYP enzyme alone. As an advantage, the immobilized enzymes reside in conditions close to the *in vivo* situation. The presence of surfactants is needed to immobilize microsomes to the bilayer surface (Morigaki, 2008). In this thesis, Pluronic® F-127 poloxamer will be utilized for this purpose. Pluronic block copolymers have been shown to fluidize biological membranes (Batrakova *et al.* 2001).

In the case of human liver microsomes, cross-linking is not easily applicable as the enzyme system is composed of a lipid membrane. Cross-linking microsomal vesicles as such would likely result in enzyme inactivation and uncontrollable aggregation of the microsomes, which in turn would severely limit substrate diffusion. One could, however, envision a strategy where microsomal membranes are functionalized with a linker molecule of adequate length, by utilizing for example the liposome method introduced in this thesis. By tuning the molar ratio of the linker molecule, stable cross-linked networks of HLM allowing efficient diffusion could possibly be generated. Soluble bacterial CYP enzymes have been

immobilized by cross-linking (Tan *et al.* 2015), but similar studies on soluble human CYPs could not be found.

Despite its limitations, covalent bonding has also been used in the immobilization of microsome structures. Nicoli *et al.* (2008) immobilized recombinant human CYP liposomes on a liquid chromatography (LC) column functionalized with neutravidin by labelling the CYP-liposome-structures with biotin. The constructed IMER was used to conduct on-line drug metabolism studies by coupling the system to a mass spectrometer (MS). However, the kinetic parameters of the immobilized enzyme were not discussed in the article. Moreover, the metabolite solutions had to be concentrated by LC before analysis, which implies a rather low enzyme activity. The researchers also admit that the experiments had to be conducted at room temperature, as the immobilized enzyme did not withstand elevated temperatures. This greatly undermines the method's utility in simulating *in vivo* metabolism.

Soluble recombinant CYPs, from which the hydrophobic membrane N-terminus sequence has been truncated, have been used more extensively in direct covalent immobilization (Wollenberg *et al.* 2013; Ménard *et al.* 2012; Gannett *et al.* 2006). Here bare CYPs are understandably more applicable, as the different functional groups of the amino acids are more readily available for bonding with different chemistries. One drawback of this approach is that NADPH-CPR must be introduced in solution along with the substrate separately for each reaction, which raises the operational costs considerably. Both CYPs and the redox partners could also be immobilized on the same carrier. However, the adjustment of spatial relationships and stoichiometric ratios of the different proteins might prove challenging. No examples of simultaneous immobilization of CYPs and their redox partners were found in the literature.

CYP enzymes have also been immobilized on different electrode surfaces (Schneider & Clark 2012). The utilization of electrodes in CYP immobilization can obviate the need for NADPH and NADPH-CPR as electrons can be accepted directly from the electron surface. This way CYPs can be used as biosensors by monitoring changes in current when exposing the system to different substrates.

However, it remains uncertain as to what extent does the direct electron transfer mimic the situation in solution *in vitro* or even *in vivo*.

2.3 Liposomes

2.3.1 Overview

Liposomes are spherical vesicles composed of at least one lipid bilayer. Liposomes have been for long studied as promising and efficient drug- and gene-delivery systems. A major challenge in the development of new drugs is delivering the drug to target tissues in therapeutic concentrations without toxic effects in other parts of the body. Liposomes have shown promise as selective carriers that can be used with drugs of different lipophilicities. Liposomes composed of natural phospholipids are biologically inert and weakly immunogenic, which makes them ideal for clinical use (Akbarzadeh *et al.* 2013; Immordino *et al.* 2006).

Liposomes can be classified according to their size, lamellarity and preparation method. The diameter of a liposome can vary from tens of nanometers to a couple of micrometers. On the basis of their size and the number of bilayers, liposomes can be divided into two categories: multilamellar vesicles (MLV) and unilamellar vesicles. Unilamellar vesicles comprise of only one lipid bilayer, and their typical size is in the range of 50-250 nm. Unilamellar vesicles can be further classified into small unilamellar vesicles (SUV, diameter <100 nm) and large unilamellar vesicles (LUV, diameter >100 nm). Multilamellar vesicles are onion-like structures comprising of several concentric lipid bilayers and have diameters of 1-5 µm. (Akbarzadeh *et al.* 2013; Immordino *et al.* 2006; Walde & Ichikawa 2001).

Preparing liposomes involves three basic steps: (i) drying lipids from an organic solvent, (ii) solubilizing and dispersing the lipid in aqueous media and (iii) purifying the resultant liposomes (Akbarzadeh *et al.* 2013). The final size, lamellarity and physical stability of the liposomes is largely dependent on the method of vesicle preparation (Walde & Ichikawa 2001). A typical way of preparing liposomes is to evaporate lipids to a dry film from an organic solvent

and then solubilizing the film in an aqueous buffer. This yields a relatively polydisperse suspension of vesicles with mainly large and multilamellar vesicles. The formation of MLVs is usually a first step in preparing a more defined population of smaller vesicles. Two commonly used methods in further processing of liposomes are extrusion and sonication. In the extrusion method, the MLV suspension is passed repeatedly through a polycarbonate membrane which contain pores of a defined size. Extrusion results in the formation of unilamellar vesicles of defined size depending on the membrane pore diameter. In the sonication method, the MLV suspension is treated with a probe or a bath sonicator for prolonged times. Sonication leads to the defragmentation of MLVs into small, unilamellar vesicles of diameters usually below 50 nm. The size distribution is less defined compared to extruded liposomes (Akbarzadeh *et al.* 2013; Walde & Ichikawa 2001). All mechanical treatments used during liposome preparation should be carried out at 5-10 °C above the phase transition temperature (T_m) of the lipids. Below T_m, the lipids exist mainly in a rigid, gel-like state. Above T_m, the hydrophobic chains become disordered, making the bilayer fluid and mechanically treatable (Walde & Ichikawa 2001).

2.3.2 Liposome fusion

Liposomes can also be used to engineer cell surfaces (Dutta *et al.* 2011). By fusing tailor-made liposomes functionalized with the chemical moieties of interest, biological membranes can be easily labelled with e.g. fluorescent molecules. The range of possible applications for liposome-mediated cell functionalization is practically limitless.

Membrane fusion is a central phenomenon in a vast range of biological processes, such as exocytosis, protein trafficking and fetal development. *In vivo,* membrane fusion is usually governed by specialized fusion proteins. Usually even long term contact between protein-free lipid bilayers does not result in membrane fusion. However, certain conditions have been found that enable spontaneous lipid bilayer fusion in the absence of fusion proteins (Chernomordik & Kozlov 2008; Cevc & Richardsen 1999).

The fusion pathway of protein-free lipids contain two essential intermediates: hemifusion structures and fusion pores. Hemifusion occurs when the outer layers of two lipid bilayer connect while the inner leaflets remain distinct. The connection is often a transient structure that either dissociates (kiss-and-run) or develops into a fusion pore. A fusion pore connects the aqueous volumes of both vesicles by a passage involving both the outer and inner leaflets of the membrane (Chernomordik & Kozlov 2008; Cevc & Richardsen 1999). The fusion pathway of protein-free lipids is illustrated in Figure 4.

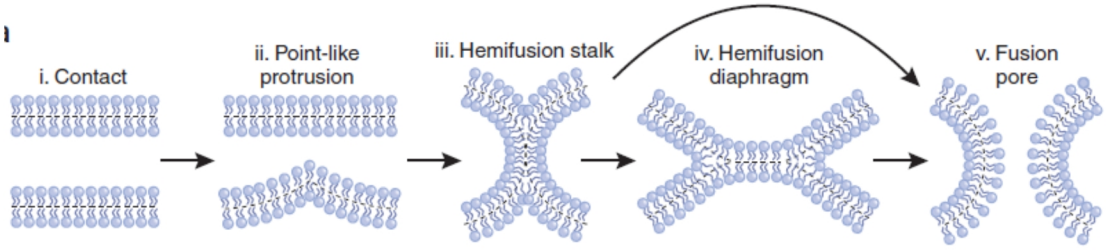

Figure 4. The fusion pathway of protein-free lipids (Chernomordik & Kozlov 2008).

The ability of lipid bilayers to form fusion intermediate states depends on lipid composition. A major factor defining the impact of given lipid on fusion propensity is its effective spontaneous curvature, meaning the curvature of a monolayer formed spontaneously by the lipid. Lipids with a positive curvature (monolayers bulged in the direction of the polar heads) tend to inhibit the formation of fusion intermediates, whereas lipids with a negative curvature promote intermediates. Fusion is also promoted by a sufficiently close contact of the two bilayers (Chernomordik & Kozlov 2008; Cevc & Richardsen 1999). Liposome contact with biological membranes can be promoted by using positively charged lipids (Bailey & Cullis 1997; Chesnoy & Huang 2000). The close contact of the membranes results in a mutual surface-charge neutralization, which further enhances the contact by the loss of water bound on the membrane surface by hydrogen bonding (Bailey & Cullis 1997). A third aspect affecting liposome fusogenicity is liposome size, with the smallest liposomes being the most fusogenic. Multilamellar liposomes are also significantly less prone to fusion than unilamellar liposomes. Increased membrane tension in small liposomes is hypothesized to drive the evolution of hemifusion structures into fusion pores (Bajoria & Contractor 1997; Malinin *et al.* 2002).

Different cell-labeling applications for fusogenic liposomes (FL) have already been introduced in the literature. Naumovska *et al.* (2014) utilized FLs in functionalizing mammalian membranes with immune cell activating lipopolysaccharides from Gram-negative bacteria. This labelling approach was proposed as a future tool for immune-based cell targeting in biomedical applications. Kleusch *et al.* (2012) introduced a rapid and efficient method for fluorescence labelling of mammalian cells using FLs. Fluorescent staining via FLs was not observed to damage the target cells in any way. Hersch *et al.* (2015) used biotin-conjugated FLs to develop an efficient cell separation mechanism based on biotin-avidin chemistry. With the developed system the researchers were able to efficiently separate fibroblasts from myocytes and cerebromicrovascular endothelial cells from fibroblasts.

2.4 Microfluidics

2.4.1 Overview

As already stated above, the miniaturization of analytical systems can offer many advantages over conventional methods. The size of the system affects various parameters. The dependence of some parameters on system size is summarized in Table 2. By decreasing the reaction volume, sample and reagent consumption can be dramatically reduced, which in turn lower cost of the analysis. The increase in surface-to-volume ratio allows for more enzyme to be immobilized per volume of the reactor. Owing to the short distances in microfluidic channels, mass and heat transfer times are dramatically reduced. In a microfluidic environment, fluid flow is laminar almost without exception, which makes the fluid dynamics well predictable and enables the generation of chemical and thermal gradients. One key benefit of microfluidic systems, that is not feasible for conventional systems, is the integration of different unit operations (e.g. reactor, separation, detection) in the same channel network, which minimizes sample loss and dead volume between the operations. As a result of the space saved by miniaturization and the advantages of microfabrication techniques, extensively parallel systems can be designed, which greatly increases the analytical throughput (Culbertson *et al.* 2014; Kovarik *et al.* 2012; Dittrich & Manz 2006).

Table 2. Dependence of reaction parameters on system size. D equals a factor of 1000 (Dittrich & Manz 2006).

Parameter	Macroscopic example	Factor change	Microfluidic example
Length of edge	1 mm	d	1 µm
Surface	1 mm^2	d^2	1 μm^2
Volume	1 mm^3	d^3	1 μm^3
Number of molecules	10^9	d^3	1
Diffusion time over d	15 min	d^2	1 ms
Linear flow	1 µm/s	d	1 mm/s
Separation time	10^5 s	d^2	100 ms

2.4.2 Microfabrication

The first miniaturized analytical systems were fabricated by etching from silicon or glass substrates. However, both of these materials have some drawbacks regarding their use in microfluidic applications. Silicon etching techniques have been well-established by the semiconductor industry, but its optical opacity hinders the use of optical detection methods. Moreover, the conductive nature of silicon prevents the use of applications utilizing an electrical field, such as capillary electrophoresis, which is the gold standard of microfluidic separation systems. Glass lacks these problems, but the microfabrication procedure is much more demanding (Franssila 2010).

Today, most of the microfluidic applications utilize polymer microfabrication for facile and low-cost microchip fabrication. The wide selection of polymers offers a vast variety of material properties, according to which the materials can be classified into three groups: hard and mechanically strong thermoplastics such as poly(methyl methacrylate) (PMMA), hard but brittle thermoset plastics such as the epoxy polymer SU-8 and soft and flexible elastomers such as

polydimethoxysiloxane (PDMS). Microfabrication techniques can be also divided into two main categories. Fabrication can either be based on replication from master or on direct machining. The direct machining methods are usually slower and need complicated instrumentation, but allow the fabrication of more complex microstructures than those feasible for replication (Holger & Gärtner 2008; Franssila 2010).

2.4.3 Microfluidics in metabolic studies

In metabolic studies, replacing conventional *in vitro* methodologies with analytical systems comprising microreactors could improve repeatability and reproducibility by replacing iterative steps and discrete sample treatment by flow injection systems. The facile implementation of system automation also helps in eliminating errors stemming from manual sample handling.

Metabolic assays utilizing immobilized enzyme microreactors can accelerate kinetic assay times significantly. Using an immobilized enzyme microreactor, substrate and inhibitor concentrations in the reactor can be changed online in a continuous manner, allowing the determination of kinetic parameters in a single run. This method has been demonstrated with e.g. protein kinase A (Cohen *et al.* 1999) and β-galactosidase (Hadd *et al.* 1997). The modular nature of microfabricated platforms also allows for easy modification of the experimental setup. For example, connecting modular microreactors in series could be used to study the interplay of different enzymes, e.g. enzymes metabolizing phase I and phase II reactions.

3 Experimental

3.1 Materials

3.1.1 Chemicals, biochemicals and enzymes

The chemicals and biochemicals used in this study are listed in Table 3. All chemicals were of analytical grade unless otherwise listed. Deionized water was purified with a Milli-Q water purification system (Millipore, Molsheim, France).

Human liver microsomes were selected as the source of CYP enzymes for immobilization because of their affordability and ease of storage. The HLM preparation used in this study was Corning® Gentest 20-Donor Pool (BD Biosciences – Discovery Labware, Woburn, MA, USA).

Table 3. Chemicals and biochemicals used in the study.

	Supplier	Purpose
Chemicals		
7-hydroxycoumarin (umbelliferone)	Sigma Aldrich, St. Louis, MO, USA	analyte
β-Nicotinamide adenine dinucleotide 2′-phosphate reduced tetrasodium salt hydrate (NADPH)	Sigma Aldrich, St. Louis, MO, USA	reagent
Biotin-PEG4-alkyne	Sigma Aldrich, St. Louis, MO, USA	reagent
Coumarin	Sigma Aldrich, St. Louis, MO, USA	analyte
Dimethyl sulfoxide (DMSO)	Sigma Aldrich, St. Louis, MO, USA	solvent
Hydrochloric acid ($HClO_4$)	Riedel-de-Haën, Seelze, Germany	reagent
Irgacure® TPO-L (old Lucirin® TPO-L) (Ethyl phenyl(2,4,6-trimethylbenzoyl)phosphinate (84434-11-7) photoinitiator	BASF, Ludwigshafen, Germany	reagent
Magnesium chloride ($MgCl_2$)	Riedel-de-Haën, Seelze, Germany	reagent
MES hydrate	Sigma Aldrich, St. Louis, MO, USA	buffer
N-(3-Dimethylaminopropyl)-N′-ethylcarbodiimide hydrochloride	Sigma Aldrich, St. Louis, MO, USA	reagent
N-hydroxysuccinimide	Sigma Aldrich, St. Louis, MO, USA	reagent
Trizma® base	Sigma Aldrich, St. Louis, MO, USA	buffer
Phosphate buffered saline, pH 7.4	Sigma Aldrich, St. Louis, MO, USA	buffer
Pluronic® F127	BASF, Ludwigshafen, Germany	reagent
Rhodamine 110	Sigma Aldrich, St. Louis, MO, USA	reagent
Biochemicals		
1,2-dioleoyl-3-trimethylammonium-propane (chloride salt) (DOTAP)	Avanti Polar Lipids, Alabaster, AL, USA	reagent
1,2-dioleoyl-sn-glycero-3-phophoethanolamine (DOPE)	Avanti Polar Lipids, Alabaster, AL, USA	reagent
1,2-dioleoyl-sn-glycero-3-phophoethanolamine-N-(Cap biotinyl) (sodium salt)	Avanti Polar Lipids, Alabaster, AL, USA	reagent
1,2-dioleoyl-sn-glycero-3-phosphoethanolamine-N-(lissamine rhodamine B sulfonyl) (ammonium salt)	Avanti Polar Lipids, Alabaster, AL, USA	reagent
1,2-dipalmitoyl-sn-glycero-3-phosphothioethanol	Avanti Polar Lipids, Alabaster, AL, USA	reagent
Streptavidin, Alexa Fluor® 488 conjugate	Life Technologies, Eugene, OR, USA	reagent

3.1.2 Microparticles and microfluidic chips

The magnetic particles used in this study were commercial paramagnetic beads (Dynabeads® M-280 or M-270, Ø = 2.8 μm) manufactured by Invitrogen / Life

Technologies (Oslo, Norway). The beads were prefunctionalized with streptavidin (M-280) or with carboxylic acid (M-270). The thiol-ene chips were fabricated and functionalized in-house. Materials used in microchip fabrication are listed in Table 4.

Table 4. Materials used in microchip fabrication.

Materials	Supplier	Purpose
1,3,5-triallyl-1,3,5-triazine-2,4,6(1H,3H,5H)-trione	Sigma Aldrich, St. Louis, MO, USA	chip fabrication
Pentaerythritol tetrakis(3-mercaptopropionate),	Sigma Aldrich, St. Louis, MO, USA	chip fabrication
Sylgard 184 base elastomer	Down Corning Corporation, Midland, MI, USA	mold fabrication
Sylgard 184 curing agent	Down Corning Corporation, Midland, MI, USA	mold fabrication
Trimethylolpropane tris(3-mercaptopropionate)	Sigma Aldrich, St. Louis, MO, USA	chip fabrication

For monitoring of microchannel packing with magnetic beads by fluorescence, 100 µL of M-270 beads was rinsed twice with 100 µL of 25 mM 2-(N-morpholino)ethanesulfonic acid buffer (MES, pH 5) for 10 min. Solutions of 50 mg/mL each of N-(3-Dimethylaminopropyl)-N′-ethylcarbodiimide hydrochloride (EDC) or N-hydroxysuccinimide (NHS) were freshly prepared in cold 25 mM MES buffer (pH 5) and 50 µL of both solutions was added to the rinsed beads and incubated with tilt rotation at room temperature for 30 min. After incubation the tube was placed on a magnet for 4 min, the supernatant was removed and the beads were washed twice with 100 µL of 25 mM MES (pH 5). After washing 60 µL of 1 mg/mL rhodamine 110 in 25 mM MES (pH 5) and 40 µL of 25 mM MES (pH 5) was added onto the beads and incubated with tilt rotation at room temperature for 30 min. After incubation the beads were washed as before.

The microchip design used in this study featured a 30x4 mm^2 array of micropillars (d=50 µm, h=200 µm). The purpose of the micropillars was to increase the surface volume of the reactor. The thiol-ene chip fabrication protocol was previously described by Tähkä *et al*. (2015). The fabrication protocol comprised four steps: (a) SU-8 master chip fabrication in cleanroom conditions, (b) casting of a polydimethylsiloxane (PDMS) mold using the SU-8 master as a template, (c) fabrication of thiol-ene channel and cover layers using the PDMS mold and (d) bonding of the thiol-ene layers. SU-8 masters were prefabricated by Dr. Ville

Jokinen, Department of Materials Science and Engineering, School of Chemical Technology, Aalto University. The PDMS molds were prepared by mixing the elastomer and the curing agent in a ratio of 1:10 (w/w). After degassing for 30 min in a desiccator, the PDMS mixture was poured onto the SU-8 master and cured at 80 °C for 3h or at 70 °C overnight. The chip fabrication protocol is illustrated in Figure 5.

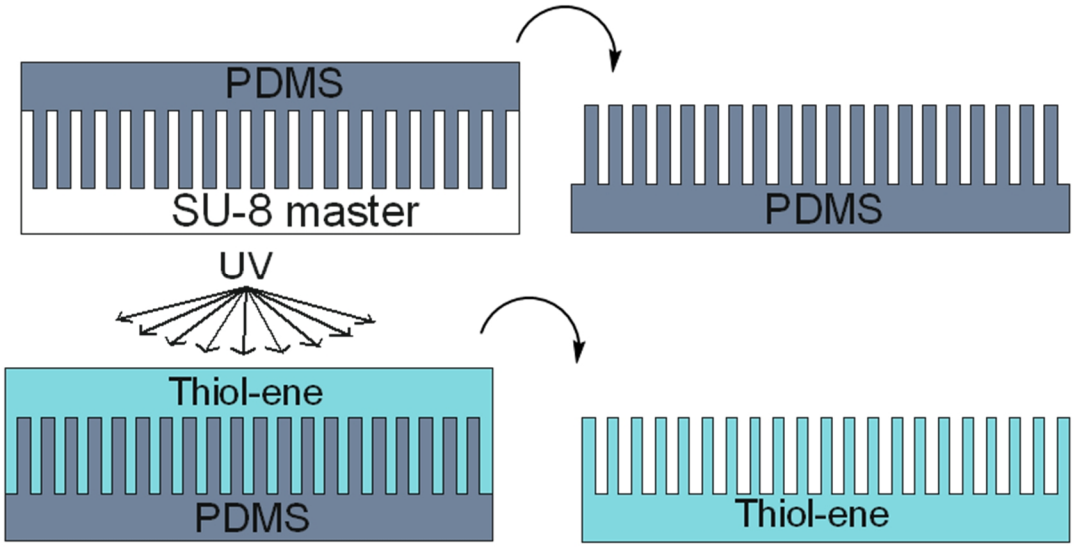

Figure 5. Schematic presentation of the fabrication steps of the thiol-ene chip (Kiiski *et al.* 2016). A PDMS mold was casted using a pre-fabricated SU-8 master. The thiol-ene layers were then casted against the PDMS and cured using UV light.

For functionalization with lipids, thiol-ene chips were fabricated by mixing two monomers, trimethylolpropane tris(3-mercaptopropionate) ("thiol") and 1,3,5-triallyl-1,3,5-triazine-2,4,6(1H,3H,5H)-trione ("ene") in a molar ratio of 2:3 with respect to free thiol and allyl groups, resulting in a allyl-rich surface which enabled chip functionalization with thiol-containing lipids. For streptavidin-functionalization, pentaerythritol tetrakis(3-mercaptopropionate) was used as the thiol monomer with a molar ratio of 3:2 with respect to free thiol and allyl groups, resulting in a thiol-rich surface which enabled chip functionalization with alkyne-containing biotin. After mixing, the monomer mixture was poured onto the PDMS mold and the molds were kept under vacuum for 5 min to facilitate the filling of the cavities on the PDMS molds. Next, the thiol-ene mixture was cured under a UV lamp (Dymax 5000-EC Series UV flood exposure lamp, Dymax Corporation, Torrington, CT, USA, nominal power 225 mW/cm^2) for 10 min. Both the channel and the top layer were fabricated in the same manner. Inlet and outlet holes

(Ø = 1.8 mm) were manually drilled onto the top layer with a finger drill. After curing, the two layers were laminated together after preheating the chips to 70 °C. Bonding of the layers was finalized by exposing to UV for an additional 2 min. A fabricated pillar chip with a scanning electron microscope (SEM) detail of the pillar structures can be seen in Figure 6.

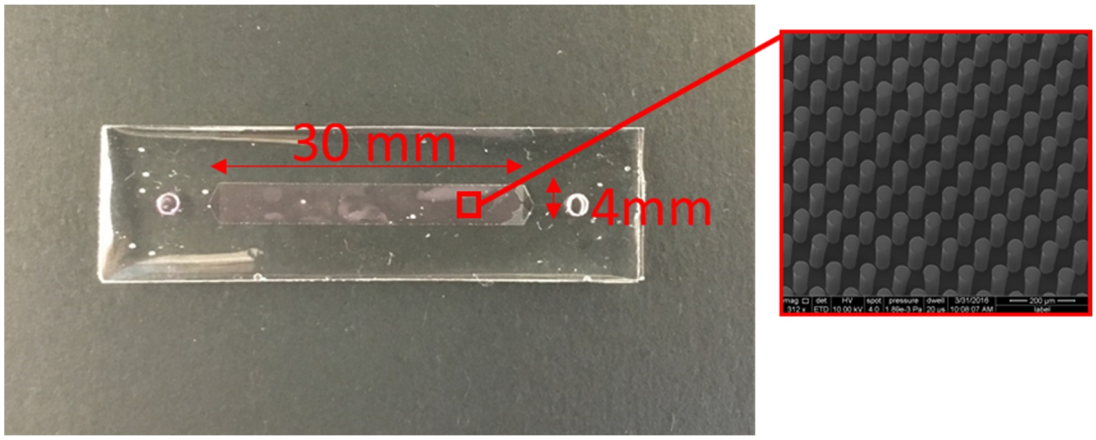

Figure 6. Photograph of the final thiol-ene micropillar chip filled with red dye and a SEM image of the micropillar array (Kiiski *et al.* 2016). Micropillar dimensions: d=50 µm, h=200 µm.

3.2 Immobilization protocols

3.2.1 Nonspecific binding of HLM on magnetic particles

Streptavidin-coated superparamagnetic beads (Invitrogen) were pre-treated according to the manufacturer's protocol and functionalized with human liver microsomes.

For HLM functionalization, the desired amount of M-280 beads was rinsed with an equal volume or at least 1 mL of PBS (phosphate buffered saline), vortexed for 5 sec and placed on a magnet for 1 min. Supernatant was discarded and the beads were resuspended in the initial volume. After pre-treatment, the beads were divided in 25 µL batches. Beads were separated by an external magnet and the supernatant was discarded. 25 µL of Tris buffer (0.1 M, pH 7.5 with 3.3 mM $MgCl_2$) and 15 µL of 10 mg/mL HLM enzyme solution were added onto the beads and the mixture was incubated at room temperature for 30 min on tilt rotation and

washed 4 to 5 times with 50 µL of PBS buffer using magnetic separation. After immobilization the beads were stored in 50 µL of PBS buffer.

3.2.2 Immobilization of HLM on magnetic particles using biotinylated liposomes

Biotinylated large unilamellar vesicles were prepared according to Hersch *et al.* (2015). To prepare biotin-containing fusogenic liposomes, DOPE, DOTAP, biotin-cap-DOPE and lissamine rhodamine B-DOPE stock solutions in chloroform were mixed in a weight ratio of 1:1:0.1:0.05, respectively. After mixing the bulk solvent was evaporated with a gentle stream of nitrogen. To remove any solvent residues, the lipid mixture was kept in vacuum for 2 h and in a vacuum desiccator overnight. Next the lipids were solvated in PBS and vortexed for 1 hour to yield a total lipid concentration of 2 mg/mL and vortexed for 1 hour.

To prepare large unilamellar vesicles (LUVs), the liposome stock solution was passed through a polycarbonate membrane of a pore size of 100 nm at least 11 times using a benchtop extruder (Avanti Polar Lipids, Alabaster, AL, USA). The size distribution of the vesicles was determined by dynamic light scattering (DLS) using a Zetasizer APS (Malvern, Worcestershire, UK).

To fuse the biotin containing liposomes with microsomes, 100 µL of the LUV dispersion was added to 100 µL of 20 mg/mL HLM and incubated for 15 min at 37 °C.

Two different methods (method 1 and method 2) for immobilization with biotin-containing FLs were tested. In method 1, HLM was first fused with FLs and then immobilized on streptavidin coated particles (Figure 7). In method 2, the particles were coated with the biotin-containing FLs prior to their incubation with HLM.

Method 1

The desired amount of beads was pre-treated according to protocol (see section 4.2.1) and divided into 25 µL aliquots and the supernatant was discarded. 15 or 30 µL of HLM/FL-mixture (10 mg/ml and 1 mg/mL of HLM and lipids,

respectively) was added onto the beads and the mixture was incubated at room temperature for 30 min on tilt rotation and washed 4 to 5 times with 50 µL of PBS using magnetic separation. After immobilization the beads were stored in 50 µL of PBS buffer.

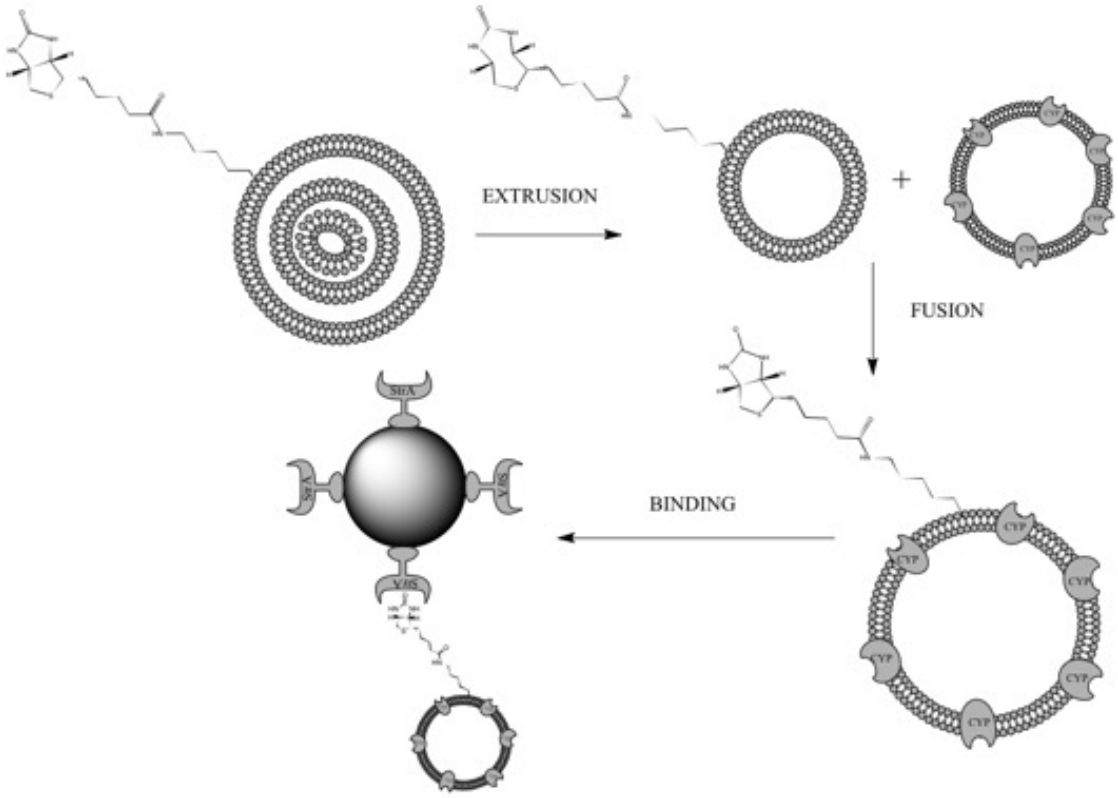

Figure 7. Schematic of HLM immobilization on streptavidin-coated magnetic particles using biotin-containing fusogenic liposomes.

Method 2

Desired amount of beads was pre-treated according protocol (see section 4.2.1) and the supernatant was discarded. An equal volume of 1 mg/mL FL mixture was added onto the beads and incubated for 30 min at room temperature. Next, the beads were divided into 25 µL aliquots, the supernatant was discarded and either 15 or 30 µL of 10 mg/mL HLM was added. Samples were incubated for 15 min on tilt rotation and washed 4 to 5 times with 50 µL of PBS using magnetic separation. After immobilization the beads were stored in 50 µL of PBS buffer.

The immobilization yield for method 1 was determined by monitoring lissamine rhodamine B fluorescence (excitation wavelength 560 nm, emission wavelength 583, bandwidth 12 nm, measurement time 100 ms) using a Varioskan Flash microplate reader (Thermo Scientific, Vantaa, Finland) from the washing fractions collected after immobilization. A standard curve was prepared from the HLM-FL-mixture by diluting with PBS. HLM was assumed to immobilize in the same proportion as the lipids. Because method 1 was selected for further studies after preliminary experiments, the immobilization yield of method 2 was not determined.

3.2.3 Immobilization of HLM in thiol-ene pillar channels

After fabrication, the thiol-ene pillar chips were functionalized with either a thiol-containing lipid (1,2-dipalmitoyl-sn-glycero-3-phosphothioethanol) or a biotinylated PEG4 alkyne (biotin-PEG4-alkyne). In the case of lipid functionalization, the chips were fabricated with a 50% molar excess of allyl groups, and in the case of biotin functionalization, a 50% molar excess of thiol groups was used. After biotin functionalization, the channel surface was further coated with a fluorescently labelled streptavidin. HLM fused with biotin-containing liposomes (protocol described in section 4.2.2) was then bound to the streptavidin molecules.

For lipid functionalization, the channels were filled with 10 mM 1,2-dipalmitoyl-sn-glycero-3-phosphothioethanol containing 1% Lucirin photoinitiator in ethanol and kept under UV for 2 min. Next, the pillar channel was rinsed with 500 µL ethanol and 500 µL 0.1 M Tris (pH 7.5, 3.3 mM $MgCl_2$) and filled with a 10 mg/mL HLM solution containing 1% Pluronic® F127 and incubated for 1h at room temperature. After incubation, the channel was washed with 0.1 M Tris (pH 7.5, 3.3 mM $MgCl_2$). The first 3 fractions (100 µL) of the washing solution were collected, after which the channel was washed with an additional 500 µL of washing buffer. The CYP2A6 activity of the collected washing fractions was determined according to the protocol described in section 4.3.1, and the amount of immobilized enzyme was evaluated by comparing the enzyme activities to the activity of a control of known enzyme concentration. Activities with respect to mg of enzyme were assumed to be identical between the control and the samples.

As a negative control, HLM were also immobilized onto the bare allyl-rich surface without prior lipid functionalization. In this case, no Pluronic® F127 was added to the HLM before incubation. The lipid functionalization protocol is illustrated in Figure 8.

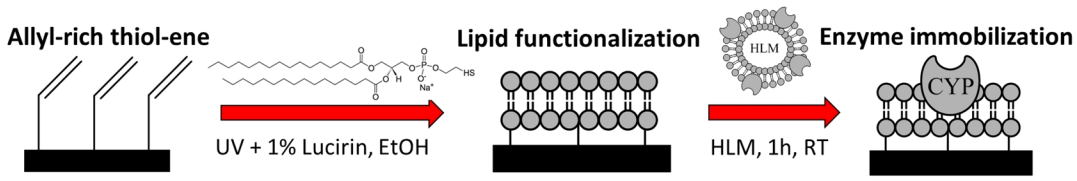

Figure 8. Schematic of the lipid functionalization of thiol-ene pillar channels (Kiiski *et al.* 2016).

For biotin functionalization, the channels were filled with 10 mM (biotin-PEG4-alkyne containing 1% Lucirin photoinitiator in DMSO and kept under UV light for 2 min. Next, the pillar channel was rinsed with 1 mL of PBS and filled with 0.66 mg/mL Alexa Fluor® Streptavidin in PBS and incubated for 45 min at room temperature. After incubation, the channels were washed with 1 mL of PBS and loaded with liposome-HLM mixture (1 and 10 mg/mL of lipids and HLM, respectively) and incubated for 30 min. After incubation, the channel was washed and the CYP2A6 activity of the wash fractions was determined in similar manner as in the lipid functionalization protocol. The biotin-streptavidin functionalization protocol is illustrated in Figure 9.

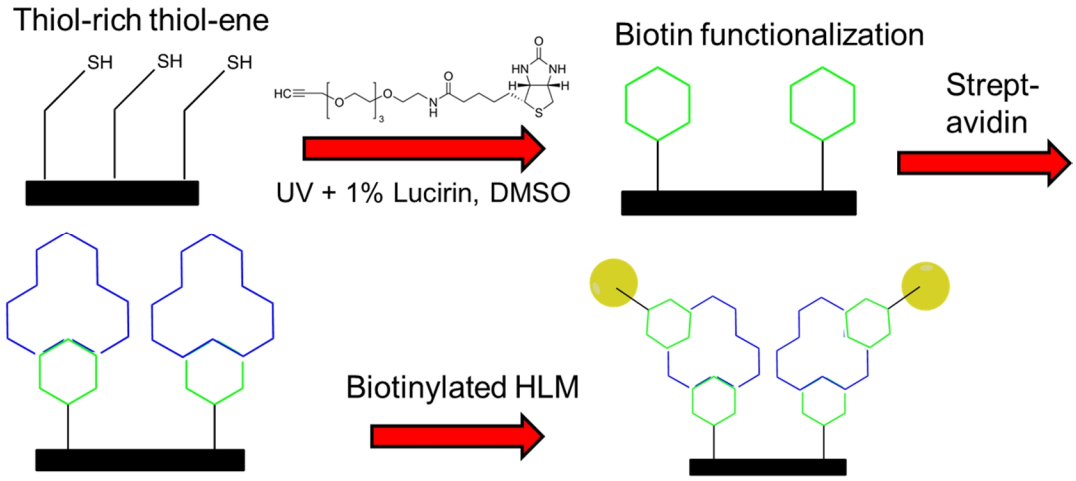

Figure 9. Schematic of the biotin-streptavidin functionalization of thiol-ene pillar channels.

3.3 Enzyme activity assays

3.3.1 Enzyme incubations

For method development, coumarin 7-hydroxylation *via* CYP2A6 (Figure 10) was selected as the model CYP activity in HLM. CYP2A6 was selected because it can be easily and specifically assayed using fluorescence spectroscopy. Coumarin by itself is non-fluorescent, but umbelliferone emits a strong fluorescence in the blue region of the visible spectrum (Fink & Koehler 1970). The fluorescence can be readily and selectively monitored even by simple well-plate methods. CYP2A6 is the only CYP isoenzyme catalyzing coumarin metabolism (Pelkonen *et al.* 2000), which allows for quantitative comparison of the different immobilized enzyme systems.

Figure 10. CYP2A6 mediated 7-hydroxylation of coumarin.

Enzyme incubation with soluble enzymes

Control enzyme activity assays were conducted in Tris buffer (0.1 M, pH 7.5 with 3.3 mM $MgCl_2$) in a total volume of 100 µL. NADPH was used as a cofactor at 1 mM. Enzyme concentration had been previously optimized to 0.4 mg/mL. Enzyme and substrate were mixed and preincubated for 5 min at 37 °C. Reactions were initiated by pipetting the cofactor into the preincubated reaction mixtures. Reactions were stopped by the addition of 1/10 of the reaction volume of 4 M perchloric acid ($HClO_4$). Samples were kept on ice for 20 min and centrifuged at 16 000 g for 10 min.

Enzyme incubation on magnetic beads

Enzyme activity assays for enzyme immobilized on magnetic particles were conducted in Tris buffer (0.1 M, pH 7.5 with 3.3 mM $MgCl_2$) in a total volume of 100 µL. NADPH was used as a cofactor at 1mM. 0.25 mg of particles were used per reaction. The magnetic particles were separated from washing buffer by an external magnet and the supernatant was discarded. The beads were then mixed with buffer and substrate and pre-incubated for 5 min at 37 °C. Reactions were initiated by pipetting the cofactor into the pre-incubated reaction mixtures. Reactions were stopped by separating the beads with an external magnet and collecting the supernatant for further analysis. The beads were washed once with 50 µL of PBS and stored at 4 °C in 50 µL PBS.

Enzyme incubation on mircrofluidic devices

The CYP activity of the immobilized enzyme reactors was assessed by pumping a reaction solution containing 1 mM of NADPH and 50 µM of coumarin in Tris buffer (0.1 M, pH 7.5 with 3.3 mM $MgCl_2$) through the reactor at different flow rates using a programmable syringe pump and monitoring the coumarin-7-hydroxylation rate off-line from the collected fractions. Solutions were fed and collected through Teflon® capillaries connected to the chip *via* NanoPort connectors (Upchurch Scientific). NanoPort connectors were fastened to the chip using 3D-printed holders fabricated and designed in-house. The reactors were heated to physiological temperature using a resistive heater (R = 0.5 Ω)

connected to an external voltage source (heating power 0.6–0.8 W). Temperature was measured from the top surface of the chip with a thermocouple connected to a multimeter. On the basis of a prior work (Sikanen *et al.* 2008), the temperature on the chip surface was approximately 2 degrees lower than that inside the channel and thus the measured temperature was targeted at 35 °C. A picture of the IMER setup can be seen in Figure 11.

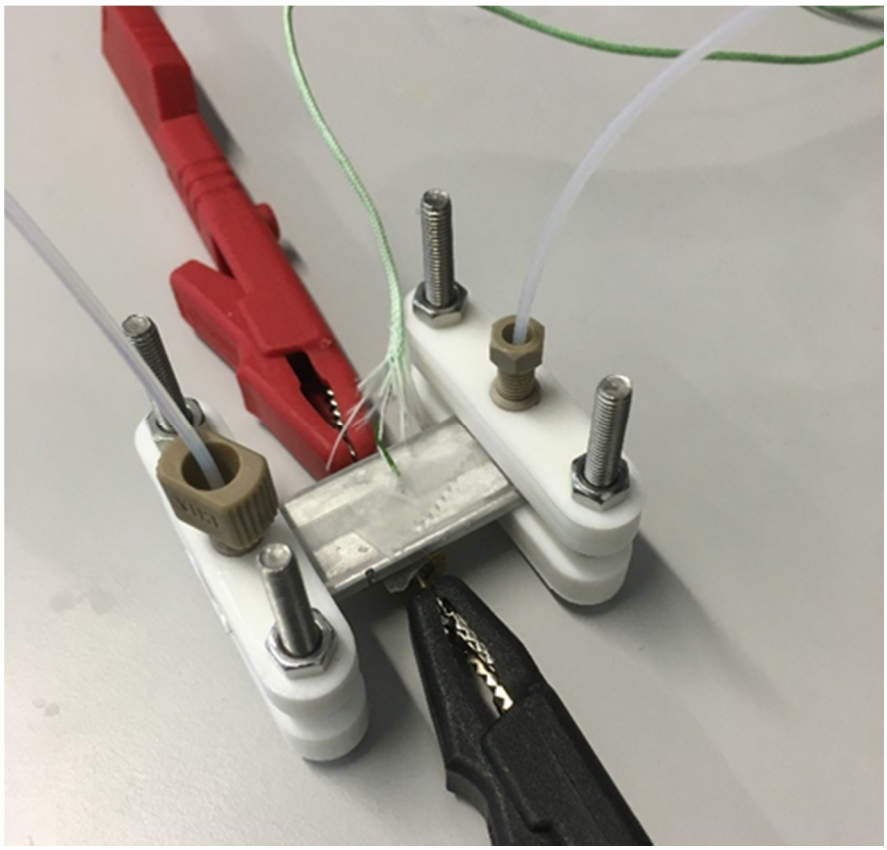

Figure 11. Photograph of the experimental IMER setup with fluidic couplings, a resistive heater and a thermocouple for recording the temperature on the reactor's top surface (Kiiski *et al.* 2016).

3.3.2 Metabolite quantitation

Umbelliferone was quantitated by fluorescence spectroscopy (excitation wavelength 325 nm, emission wavelength 470 nm, bandwidth 12 nm, measurement time 100 ms) using a Varioskan Flash microplate reader (Thermo Scientific, Vantaa, Finland). As NADPH gave a considerable fluorescence signal in neutral pH, all neutral samples were acidified prior to analysis by adding 1/10 of sample volume of 4 M $HClO_4$.

4 Results

4.1 HLM Stability and characterization

In order to confirm the stability of HLM over time periods required for immobilization protocols, the enzyme activity was determined over a period of 120 min from a HLM sample stored at room temperature. Results are shown in Figure 12. According to the results, HLM activity did not significantly drop over short storage periods of time at room temperature.

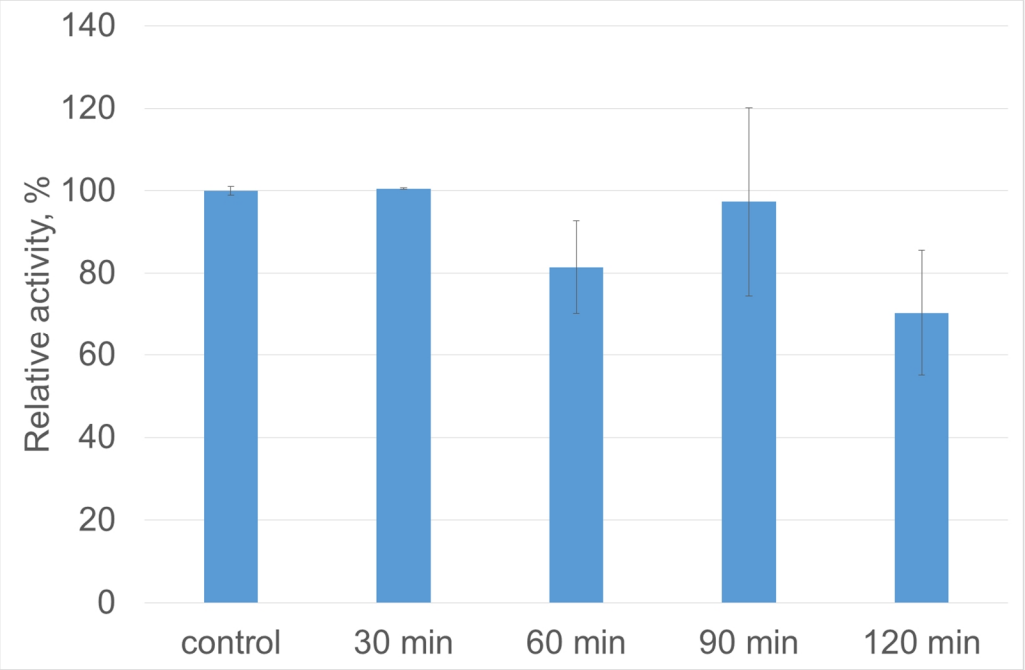

Figure 12. Relative CYP2A6 activity (coumarin 7-hydroxylation) of HLM stored at room temperature. The error bars represent one standard deviation from the mean. n=2

To examine how the enzyme activity of HLM is preserved over extended storing periods, enzyme activity of HLM stored in the fridge (4°C) was determined over a period of 9 days according to the protocol described in section 4.3.1. Results are shown in Figure 13. It should be noted that as the microparticles do not tolerate freezing (Anon. 2016a), the HLM-functionalized beads should be stored at 4 °C. According to the results, HLM can be stored for extended periods at 4 °C without significant loss of enzyme activity.

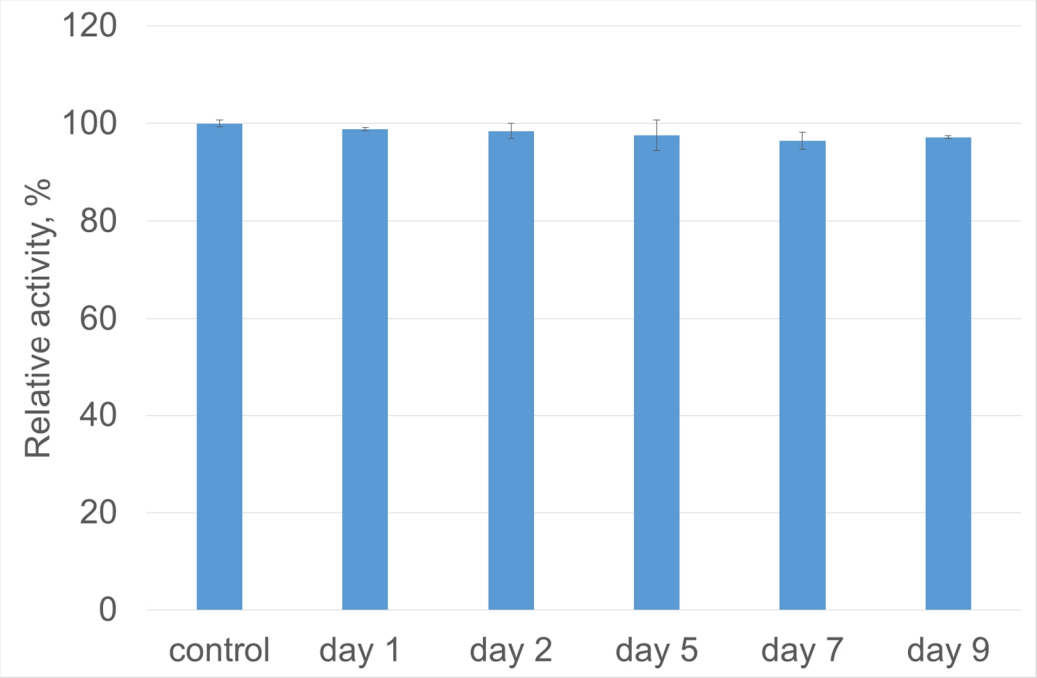

Figure 13. Relative CYP2A6 activity (coumarin 7-hydroxylation) of HLM stored at 4 °C. The error bars represent one standard deviation from the mean. n=2

To assess the influence of thermal inactivation on the loss of enzyme activity in immobilized enzymes, a 4 mg/mL solution of HLM was incubated at 37 °C and on designated time points 10 µL of the enzyme was added to a reaction solution. Next, the assay was carried out as per protocol described in section 4.3.1. As can be seen from the results (Figure 14), bare HLM in solution tolerates incubation in physiological temperatures reasonably well without any significant thermal inactivation. This must be taken into account when assessing the possible reasons for activity loss when using immobilized HLM.

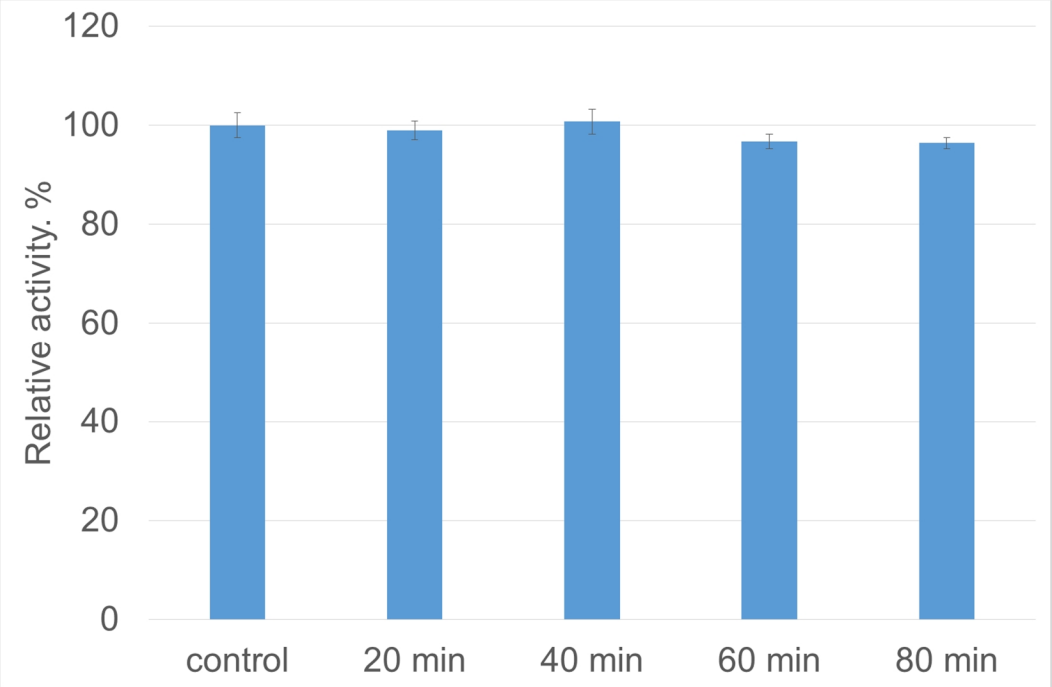

Figure 14. Relative CYP2A6 activity (coumarin 7-hydroxylation) of HLM incubated at 37 °C. The error bars represent one standard deviation from the mean. n=2.

The zeta potential and vesicle size distribution of stock HLM solution was measured with Zetasizer Nano ZS (Malvern, Worcestershire, UK) using a HLM concentration of 0.125 mg/mL in de-ionized water. The size distribution of HLM can be seen in Figure 15. According to the data, HLM is distributed to three distinct fractions by vesicle diameter. The zeta potential of HLM was measured to be -44.3 mV. As discussed in the literature review (section 2.3), the negative charge of the HLM membrane surface promotes the close contact between HLM and FL as a result of electrostatic interactions.

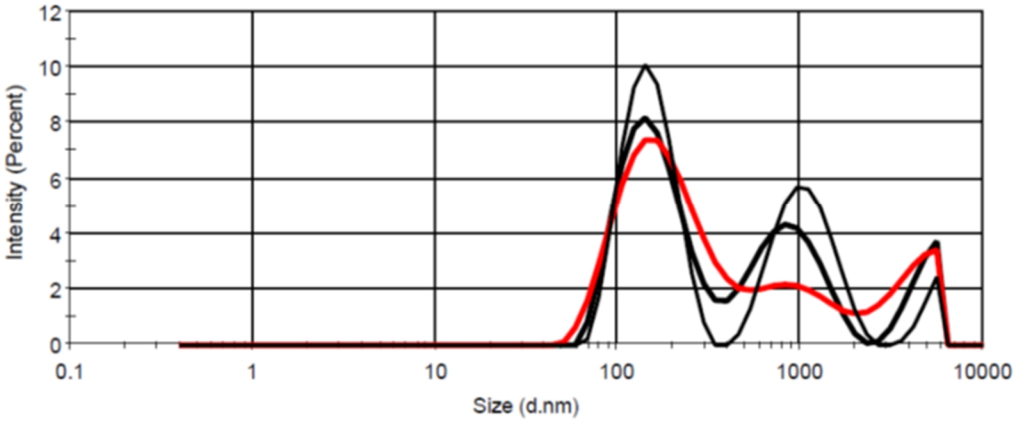

Figure 15. Size distribution by scattering intensity of HLM according to dynamic light scattering measurements.

4.2 Liposome preparation and fusion with HLM

The decrease in liposome size after extrusion was monitored both microscopically and with dynamic light scattering analysis. The size distribution data from the dynamic light scattering measurements before and after extrusion are shown in Figure 16. The polydispersity index (PDI) of the liposome solution decreased from 0.176 to 0.094 as a result of the extrusion process. The z-average value, which denotes the average hydrodynamic radius of the sample particle population, decreased from 662 nm to 240 nm. It should be noted that because the z-average gives only a single average value for the whole particle population, it does not accurately describe the size distribution of the polydisperse pre-extrusion sample.

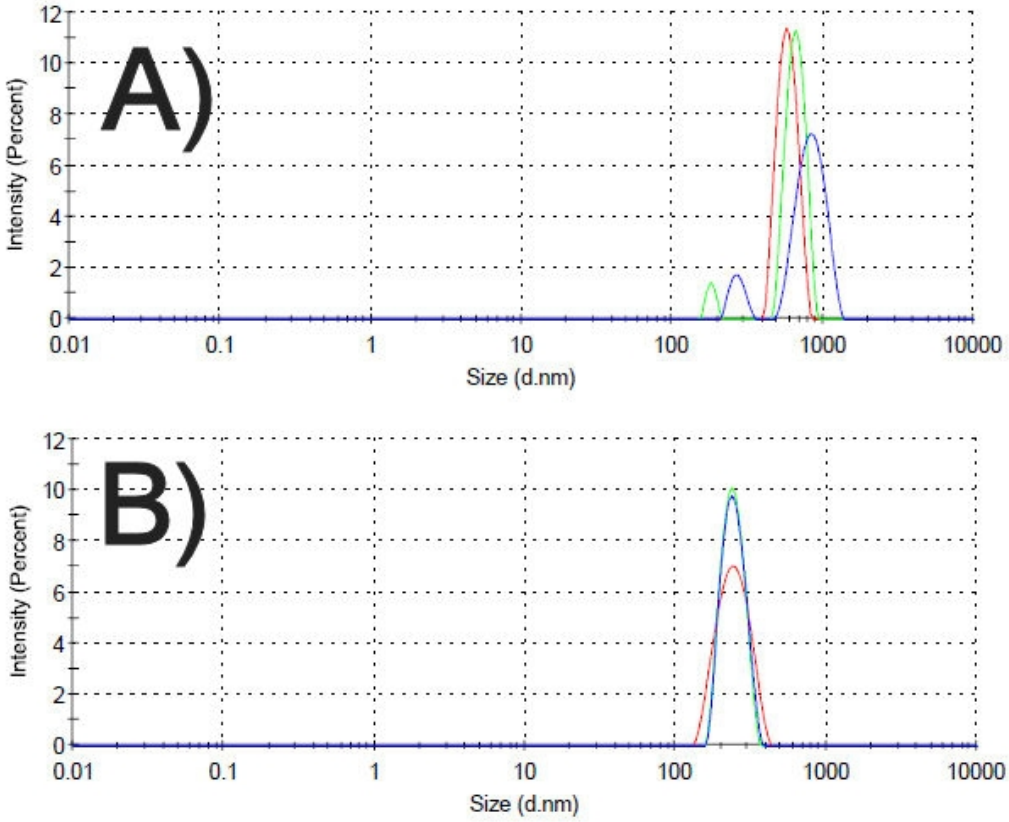

Figure 16. Size distribution of fusogenic liposome solution by scattering intensity according to dynamic light scattering measurements A) before extrusion B) after extrusion (51x through a 100 nm membrane).

The liposome samples were imaged using a microscope (Zeiss Axio Scope A1, broadband halogen lamp with an excitation filter 546 ± 5 nm and an emission filter 545-700 nm) by exploiting the fluorescence originating from the lissamine rhodamine B derivatized lipids. Microscopic images of the liposomes before and after the extrusion are shown in Figure 17. The drop in the average size of the liposomes was apparent from the pictures.

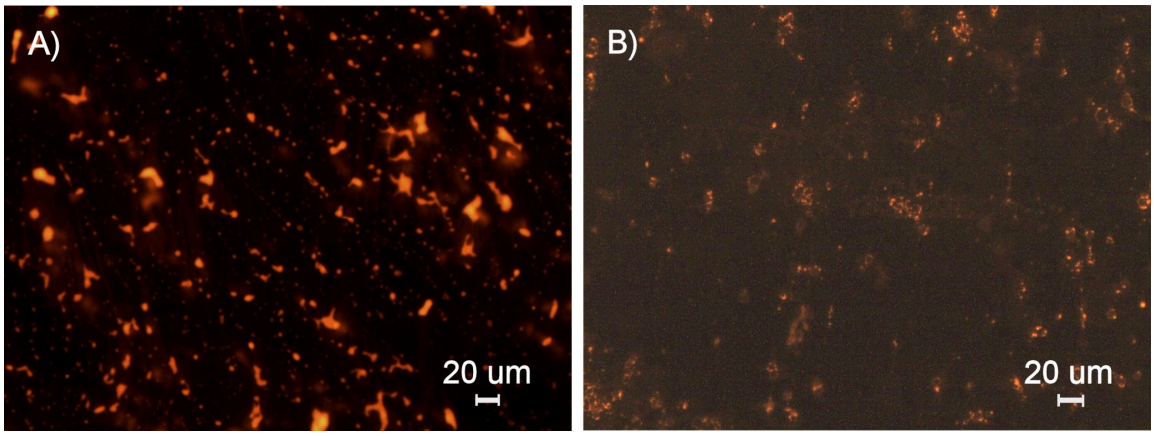

Figure 17. Fusogenic liposomes A) before extrusion B) after extrusion (50 x through a 100 nm membrane) visualized using lissamine rhodamine B fluorophore. Magnification 20x, excitation wavelength 546 nm, emission wavelength 583 nm.

After fusing the HLM with the fusogenic liposomes, the mixture was again examined microscopically (Figure 18). The fluorescence signal can be seen enriched on the surface of the microsomal membranes.

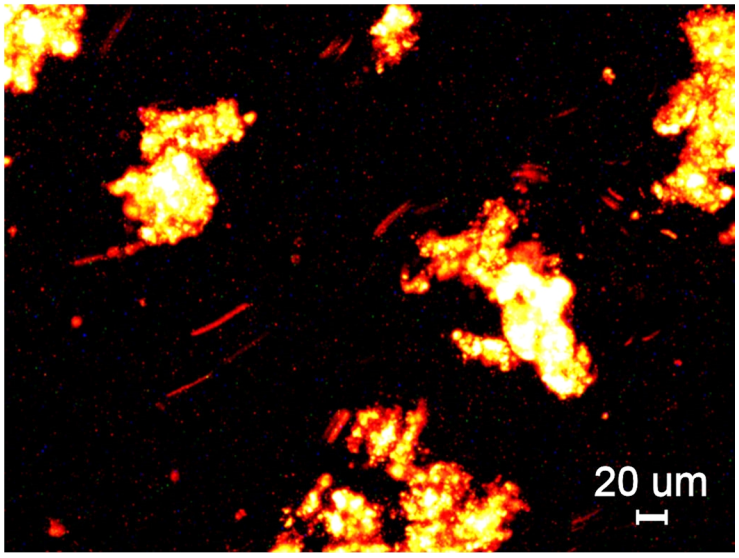

Figure 18. HLM fused with fusogenic liposomes visualized using lissamine rhodamine B fluorophore. Magnification 20x, excitation wavelength 546 nm, emission wavelength 583 nm.

4.3 Immobilization of HLM on magnetic microparticles

4.3.1 Nonspecific method

The nonspecific adsorption of HLM on streptavidin-coated magnetic microparticles was first used to roughly optimize the immobilization conditions in terms of the enzyme vs. particle ratio and the incubation volume during immobilization.

First, the effect of incubation volume during immobilization was assessed by changing incubation volume from “small” to “large” using two different enzyme-to-particle ratios, 1:1 (volumes of 25 and 100 µL) and 2:1 (volumes of 50 and 100 µL). According to the results (Figure 19), the incubation volume during immobilization does not significantly affect the CYP2A6 activity of the immobilized HLM. On these grounds, results from experiments using different immobilization volumes could be compared with each other.

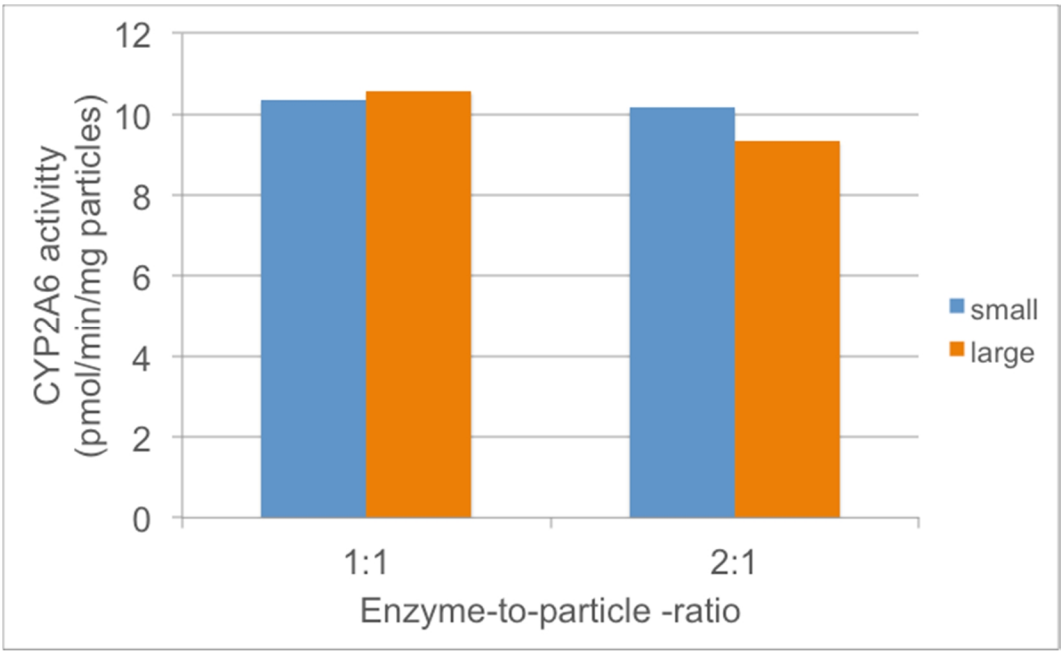

Figure 19. The effect of incubation volume during immobilization (25/50 vs. 100 µL) on sample CYP2A6 activity (coumarin 7-hydroxylation) with two different enzyme-to-particle ratios.

With the tested ratios, the enzyme-to-particle ratio had no effect on CYP2A6 activity of the immobilized HLM (Figure 20). This is likely because the adsorption of HLM on the particles saturates at very low levels of enzyme. Enzyme consumption per particle sample was minimized based on these results to lower enzyme consumption.

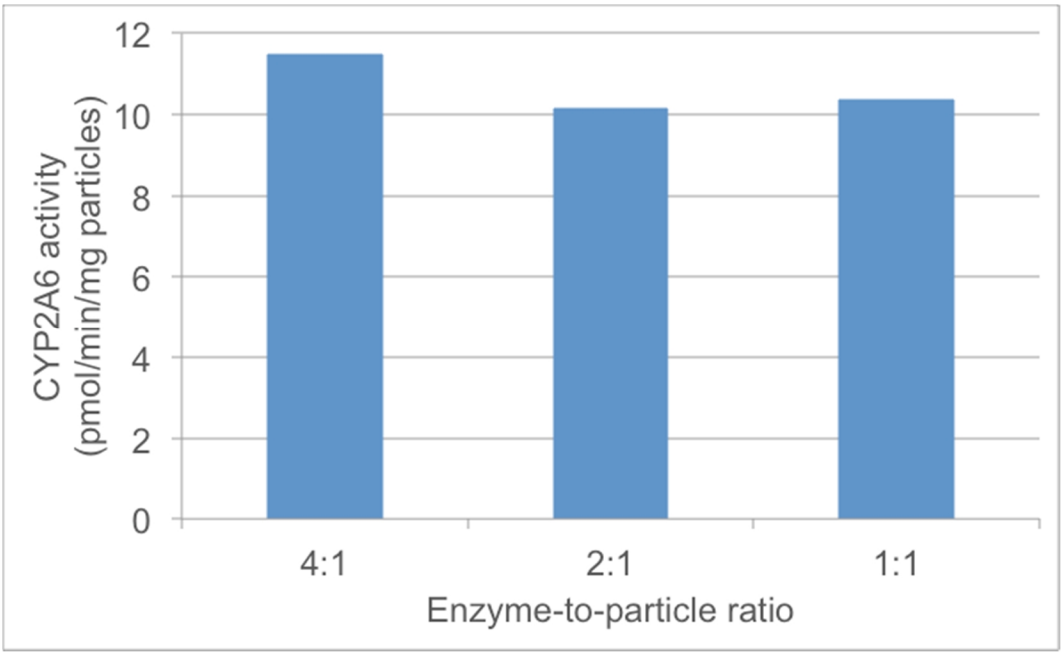

Figure 20. The effect of enzyme-to-particle ratio during immobilization on sample CYP2A6 activity (coumarin 7-hydroxylation). n=1 particle batch.

The effect of the amount of particles used for immobilization (at fixed HLM amount of 1 mg total protein) was also examined. According to the results, the CYP2A6 activity of the samples with respect to mg of particles is not significantly affected by the amount of particles used (Figure 21). Thus, 0.25 mg of beads per sample was used in further experiments to minimize bead consumption.

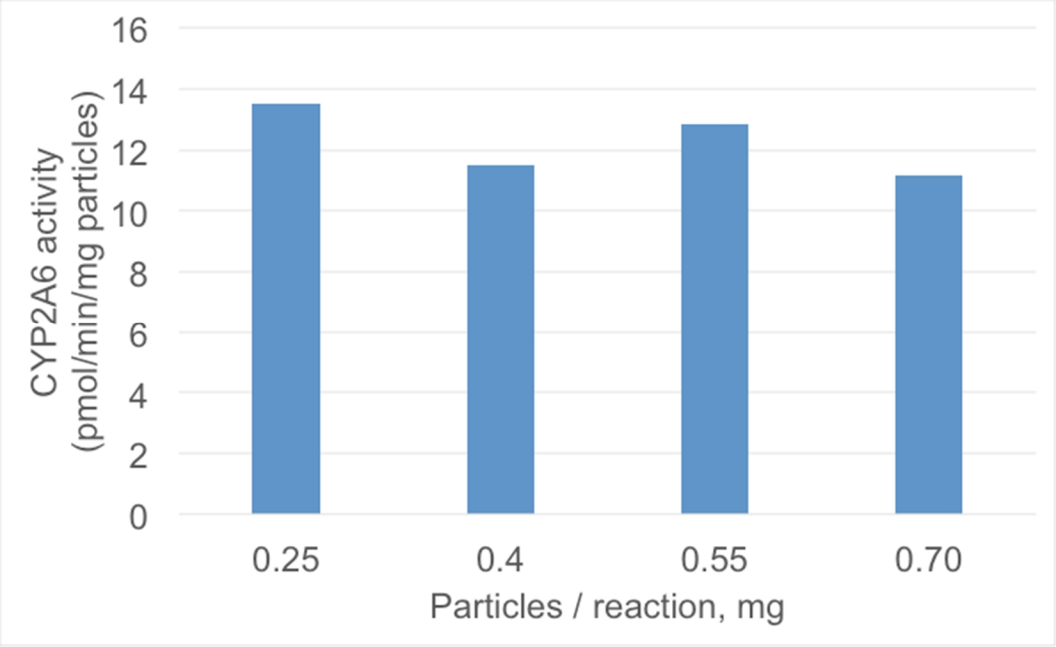

Figure 21. The effect of particle amount in immobilization on the CYP2A6 activity (coumarin 7-hydroxylation) of the samples. n=1 particle batch.

An attempt was made to determine the immobilization yield of the nonspecific immobilization method by measuring the amount of non-immobilized HLM with the bicinchonic acid (BCA) assay (Thermo Scientific, Rockford, IL, USA). However, the sensitivity of the assay was not adequate for determining such minute enzyme concentrations, as the inter-sample variation was greater than the concentrations to be measured.

To assess the effect of immobilization on enzyme kinetics, the Michaelis-Menten kinetic parameters (V_{max} and K_m) for coumarin 7-hydroxylation were determined for the nonspecifically immobilized enzyme using coumarin concentrations of 1, 2, 4, 8, 16, 32 and 64 µM. Two parallel incubations were performed at each substrate concentration. The kinetic parameters were calculated using GraphPad Prism software (GraphPad Software Inc., CA, USA). The calculated V_{max} and K_m values were 15.2 ± 0.6 pmol/min/mg and 1.2 ± 0.25 µM respectively. The K_m values for coumarin 7-hydroxylation reported in the literature range from 0.5 to 2.0 µM (Yuan *et al.* 2002), which are comparable to the values determined for the immobilized HLM. It should be noted that the V_{max} value is reported in relation to mg of particles, not enzyme. Thus it cannot be directly compared with the values given for the soluble enzyme in literature. The Michaelis-Menten plot of coumarin 7-hydroxylation for the nonspecifically immobilized HLM is shown in Figure 22.

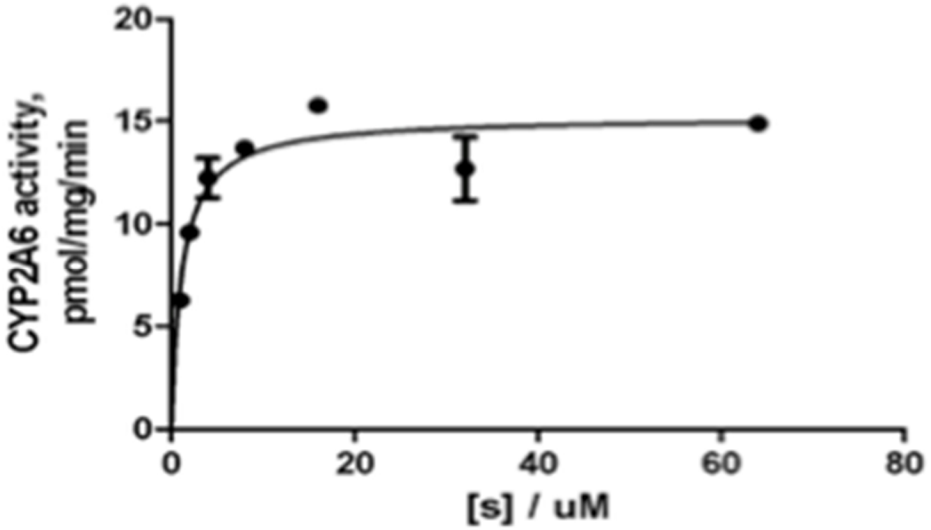

Figure 22. Michaelis-Menten plot of coumarin 7-hydroxylation for HLM nonspecifically immobilized on streptavidin-coated magnetic particles.The solid line represents the nonlinear least-squares best fit to the Michaelis-Menten equation. n=2 parallel incubations at each substrate concentration

The stability of HLM immobilized with the nonspecific method was examined by storing the particles after HLM immobilization at 4 °C and determining the enzyme activity daily over a period of 3 days. To differentiate between loss of activity during the enzyme reaction and during storage, one sample was stored at 4 °C for three days before the initial activity measurement. According to the results (Figure 23), the beads can be stored at 4 °C for extended periods of time without any significant loss of enzyme activity. Rather, the activity loss was linked to heating and stirring of the particles during the enzyme incubation.

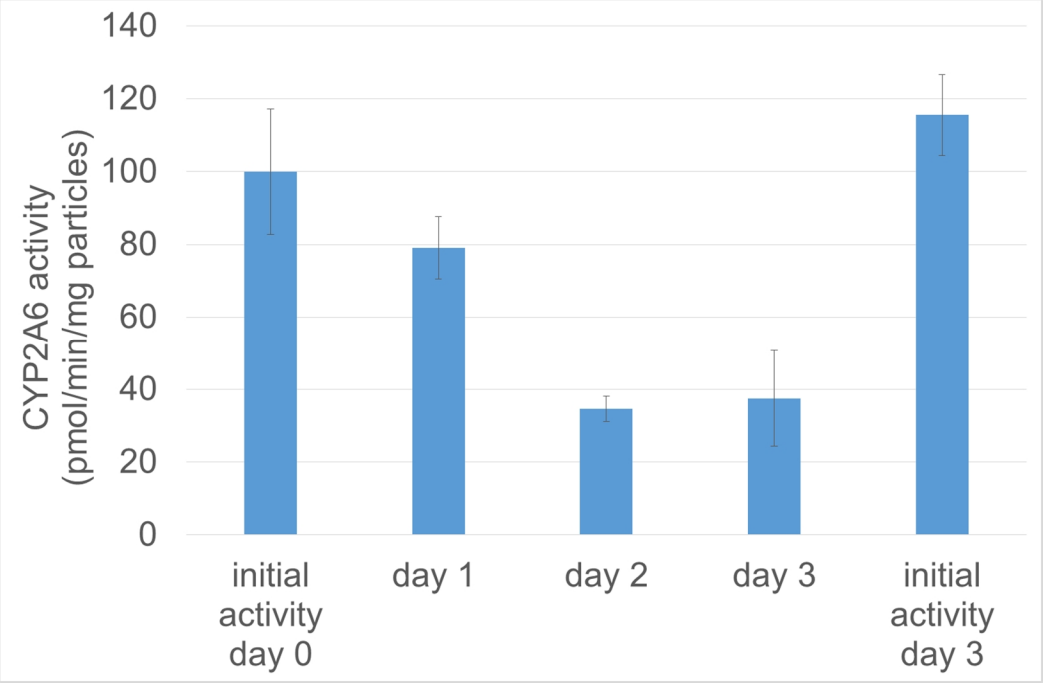

Figure 23. Relative CYP2A6 activity (coumarin 7-hydroxylation) of magnetic particles immobilized with HLM using the nonspecific method. The activity was measured on the day of immobilization and daily over a period of 3 days. One sample was stored for 3 days before enzyme activity assay. The error bars represent one standard deviation from the mean. n=4 particle batches.

To identify the critical points affecting the loss of enzyme activity over time/repeated use of particles after immobilization, the enzyme activity of wash solutions was determined (following the enzyme incubation protocol used for the soluble enzyme). To assess the effect of incubation at elevated temperatures on enzyme leaching, one sample was incubated in 37 °C for 20 min, after which the CYP2A6 activity of the supernatant was determined (see wash fraction after reaction, Figure 24). It should be noted that the assay method cannot be used to actually quantitate the amount of lost enzyme, as no standard enzyme solutions were used. The amount of generated metabolite gives only a rough estimate on the extent of enzyme loss at different points. The method also allows only the detection of active enzyme.

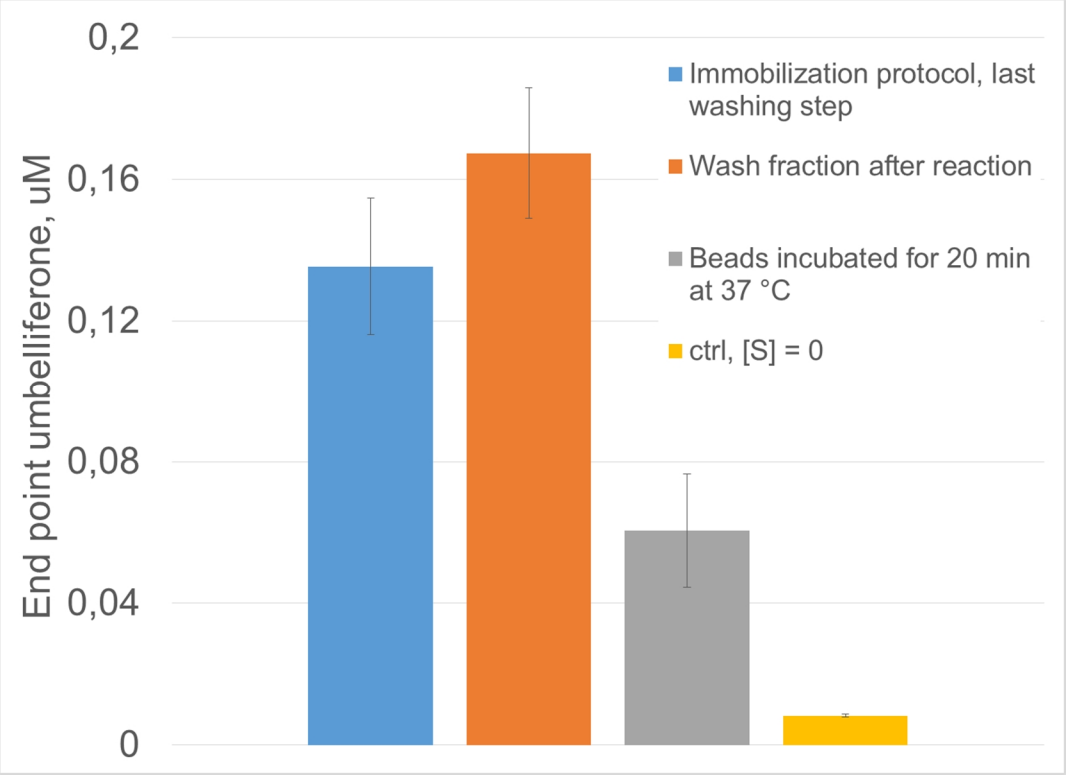

Figure 24. CYP2A6 activities (coumarin 7-hydroxylation) of washing fractions collected at different points of the immobilization/incubation protocol. n=4 particle batches.

4.3.2 Immobilization with biotinylated liposomes

To roughly assess the effect of the enzyme-to-particle ratio on immobilization efficiency, the immobilization protocol was carried out using two different ratios of particles and the HLM-FL mixture (10 mg/mL HLM, 1 mg/mL LUV). According to the results, the ratio did not affect the CYP2A6 activity of the particles (Figure 25). Compared to the nonspecific immobilization method, the utilization of FLs confers a 3-fold increase in CYP2A6 activity.

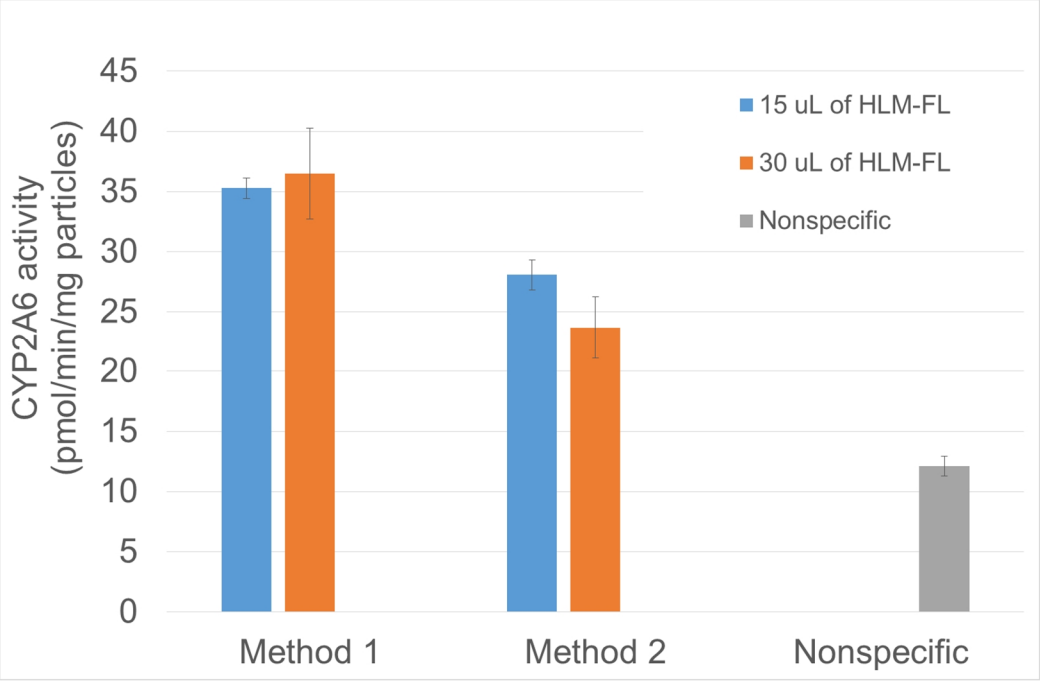

Figure 25. CYP2A6 activity (coumarin 7-hydroxylation) of magnetic particles immobilized with HLM fused with biotin-containing fusogenic liposomes (FL). Method 1: HLM fused with FL prior to immobilization, Method 2: FL immobilized on magnetic particles prior to adding HLM. Typical activity achieved with the nonspecific immobilization method is included for reference. The error bars represent one standard deviation from the mean. n=4 particle batches.

The beads immobilized with method 2 showed a noticeable change in their appearance after incubation with the liposomes. The beads had a tendency to aggregate, which may be due to changes in the bead surface charge or hydrophobicity. The aggregation resulted in rapid sedimentation of the particles. Because of this and the slightly lower activity of beads immobilized with method 2, method 1 was selected for further studies.

The stability of magnetic particles functionalized with immobilized HLM according to method 1 was assessed by measuring the initial activity after immobilization and repeating the enzyme assay twice after storing the samples for 6 days at 4 °C. Storing the samples for extended periods did not seem to effect the activity much, but after repeated incubations, the activity started to diminish (Figure 26).

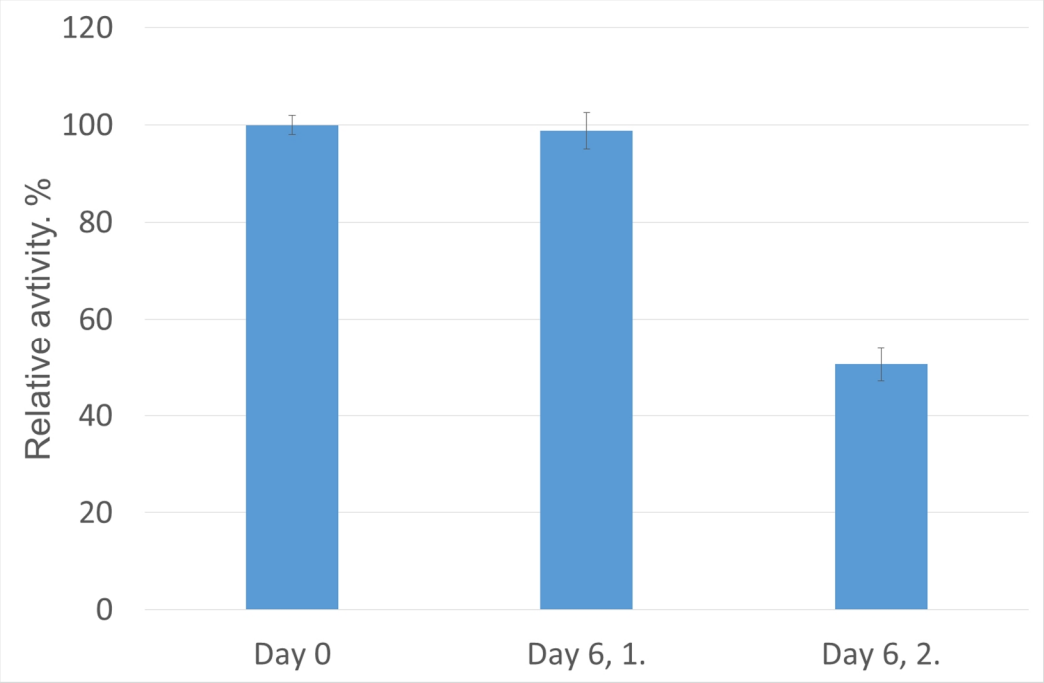

Figure 26. Relative CYP2A6 activity (coumarin 7-hydroxylation) of magnetic particles immobilized with HLM fused with biotin-containing fusogenic liposomes (FL). The activity was measured on the day of immobilization and twice after six days of storing at 4 °C. The error bars represent one standard deviation from the mean. n = 4 particle batches.

The Michaelis-Menten kinetic parameters were determined in a similar manner to the nonspecific method. Two parallel incubations were performed at each substrate concentration The calculated V_{max} and K_m values were 24.3 ± 1.1 pmol/min/mg and 2.5 ± 0.49 µM respectively. The K_m value for CYP2A6-mediated coumarin 7-hydroxylation is reported to be 0.5-2 µM in the literature (Yuan *et al.* 2002), which is comparable to the values determined for the immobilized HLM. The Michaelis-Menten plot of coumarin 7-hydroxylation for the nonspecifically immobilized HLM is shown in Figure 27.

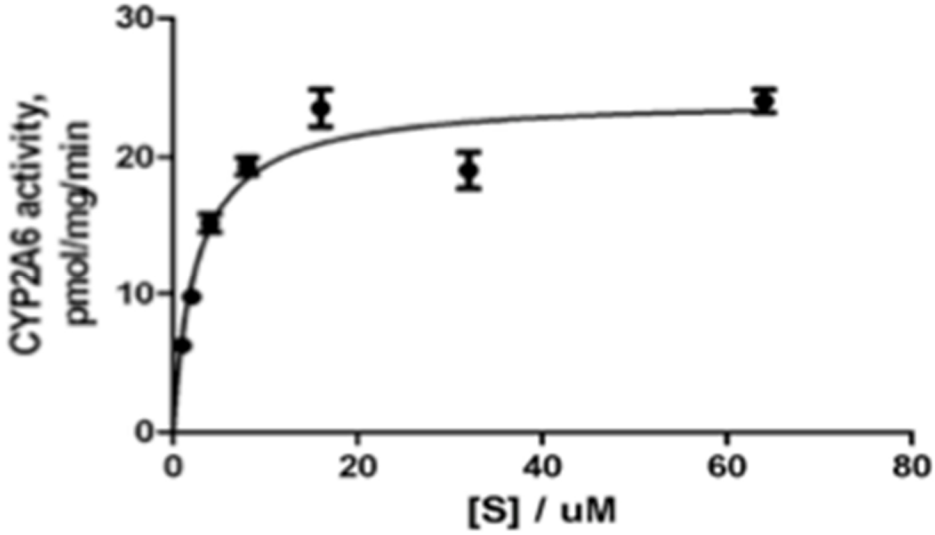

Figure 27. Michaelis-Menten plot of coumarin 7-hydroxylation for HLM immobilized on streptavidin-coated magnetic particles using biotin-containing liposomes. The solid line represents the nonlinear least-squares best fit to the Michaelis-Menten equation. n=2 parallel incubations at each substrate concentration.

The immobilization yield of method 1 was determined by measuring lissamine rhodamine B fluorescence (excitation wavelength 560 nm, emission wavelength 583) from the washing fractions collected after immobilization and subtracting the measured lipid content from the amount of lipids used in the immobilization. The BCA assay was not used, as the excitation of lissamine rhodamine B present in the samples would surely interfere with the assay as it is based on measuring absorbance at 562 nm (Smith *et al.* 1985). HLM was assumed to immobilize in the same proportion as the lipids. The obtained immobilization yield was 15.3%. V_{max} calculated with the corresponding enzyme content was 270 pmol/min/mg of HLM.

4.3.3 Particle packing in microfluidic channels

Packing of magnetic particles inside a microfluidic channel was briefly tested in a straight thiol-ene channel (50% allyl excess) with dimensions of 45 x 0.6 x 0.05 mm. Rhodamine 110-labelled particles (0.75 mg) were loaded inside the channel manually using a syringe. The beads were retained inside the channel by placing a neodymium block magnet (10 x 10 x 5 mm, magnetization grade N42, Supermagnete, Gottmadingen, Germany) on top of the channel. After

loading the beads, a liquid flow was initiated using a syringe pump, starting at 0.5 µL/min. Particles were monitored with a microscope using laser-induced fluorescence (LIF, argon laser 488 nm, 20mW).

Using the block magnet for bead retention resulted in generation of a relatively high backpressure as the flow was initiated. The increasing pressure eventually ejected the particles out of the channel. To prevent the generation of backpressure, another magnet configuration was tested to pack the particles more loosely in the channel. Ten neodymium block magnets (5 x 4 x 1 mm, magnetization grade N50, Supermagnete, Gottmadingen, Germany) were placed on top of the channel in a 5 x 2 configuration along the channel length, with the longer side of the magnet parallel to the sides of the channel. With this configuration, 0.75 mg of magnetic particles could be held inside the channel with a flow rate of up to 3 µL/min. Using this magnet configuration, the beads were also imaged with a confocal microscope (Leica TCS SP5 MP, blue laser, excitation wavelength 496 nm) after applying a liquid flow of 2 µL/min to study the spatial distribution of the beads. A 780 x 600 µm slab spanning the whole width (600 µm) of the channel was imaged. A 3D surface plot generated from the confocal microscopy data using Fiji image-processing software (Schindelin *et al.* 2012) is shown in Figure 28. The beads can be seen concentrated on the right side of the channel.

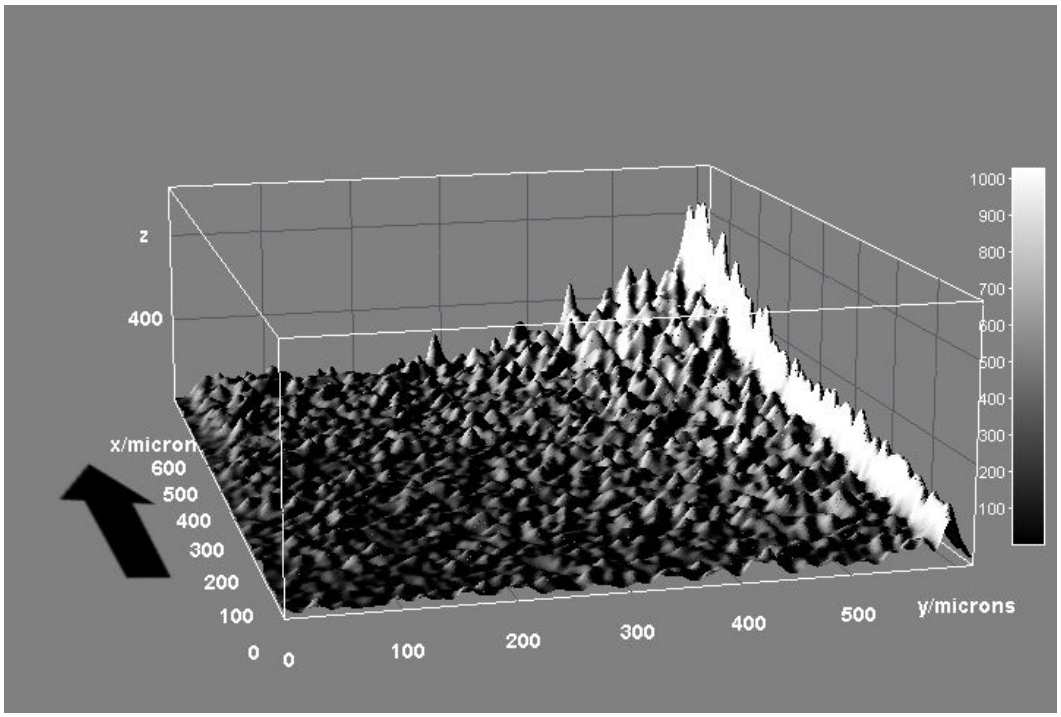

Figure 28. 3D surface plot of a generated from confocal microscopy (Leica TCS SP5 MP, 20x magnification) data on distribution of magnetic particles fixed inside a microfluidic channel using an external magnet. A 780 x 600 µm slab spanning the whole width (600 µm) of the channel is seen on the plot. The beads can be seen concentrated on the right side of the channel. The direction of flow is denoted by an arrow. Units on the Z-axis are arbitrary.

4.4 Thiol-ene CYP-IMERs

Three different methods for HLM immobilization on thiol-ene micropillar chips were studied. The thiol-ene surface was functionalized with either streptavidin or a lipid bilayer, to which HLM were subsequently immobilized. For comparison, HLM were also immobilized nonspecifically onto non-modified allyl-rich micropillars *via* physical adsorption. The immobilization yield of the different approaches was examined by determining the enzyme activity left in the washing fractions collected from the reactor after HLM immobilization. The protein contents of the collected wash fractions in relation to the amount of protein loaded to the reactor for the three different immobilization methods are shown in Figure 29. The immobilization yields for the different immobilization approaches were 33, 21 and 43% for the nonspecific, lipid-assisted and the streptavidin-biotin approach, respectively.

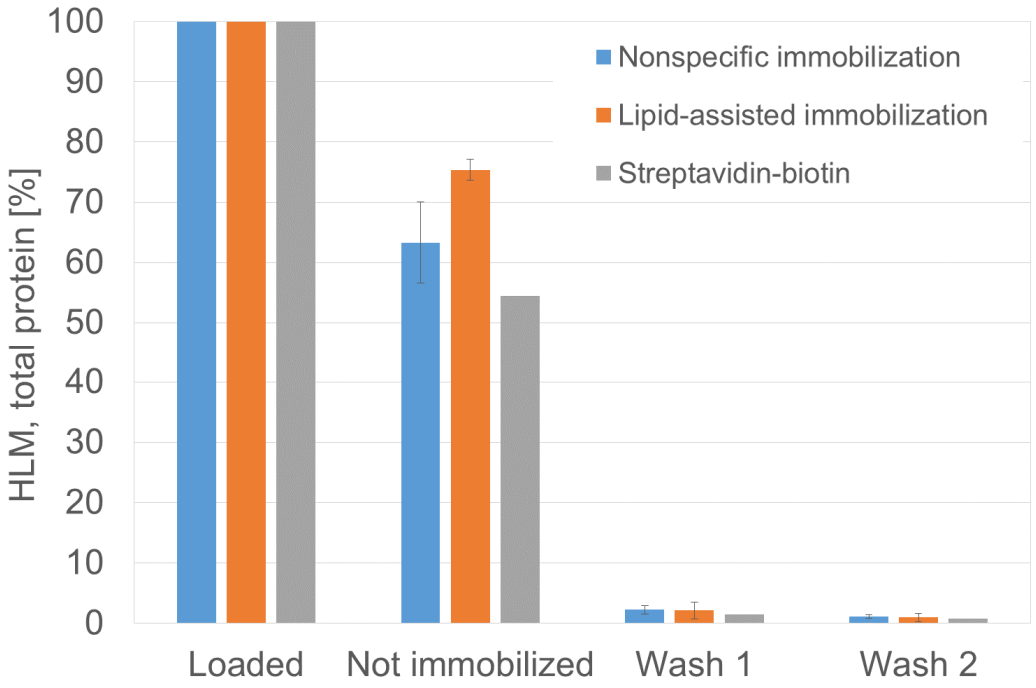

Figure 29. Relative protein content of wash fractions vs. protein amount loaded to the IMER during HLM immobilization. The error bars represent one standard deviation from the mean. n=3 reactors for nonspecific and lipid-assisted immobilization, n=1 reactor for streptavidin-biotin immobilization.

To assess the effect of flow rate on reactor activity, 50 µL fractions of the reaction solution were collected with incrementally increasing flow rates and the umbelliferone concentration of the fractions was determined. A reactor with HLM immobilized using the nonspecific method was used for this purpose. To account for the gradual loss of enzyme activity during the experiment, fractions with the initial flow rate of 5 µL/min were collected at the end of the run also. Results are shown in Figure 30. The activity of the reactor seems to decrease with increasing flow rates. As the flow rate was restored to 5 µL/min, an increase in enzyme activity was observed. Based on the results, the flow rate of 5 µL/min was selected for further studies.

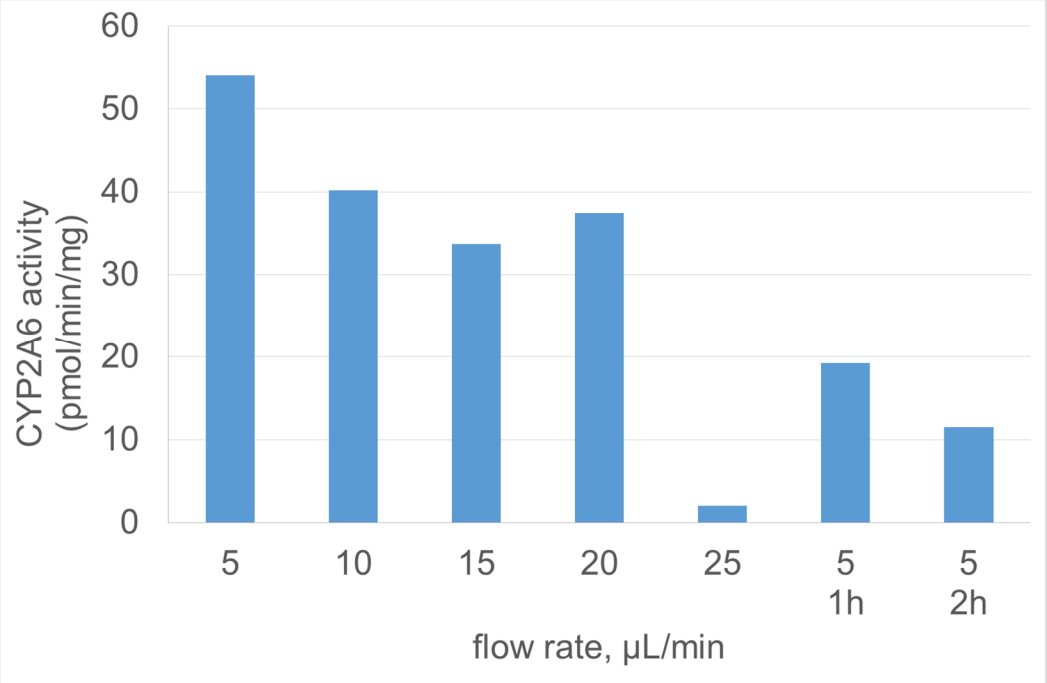

Figure 30. The effect of reaction solution flow rate on the reactor CYP2A6 activity (coumarin 7-hydroxylation). Two additional fractions with the flow rate of 5 µL/min were collected after running the reactor for 1 and 2 hours.

The activity of the IMERs was monitored by collecting 50 µL fractions of the reaction solution with a flow rate of 5 µL/min. The CYP2A6 activity of the reactors with different immobilization approaches as a function of time is shown in Figure 31. The low initial activity of the biotin-streptavidin method is due to incorrect flow rate in the beginning of the run. The average initial activities for the different immobilization approaches were 93, 51 and 32 pmol/min/mg for the nonspecific, lipid-assisted and the streptavidin-biotin approach, respectively. The activities for the nonspecific and lipid-assisted method were determined as the average from 3 individual reactors, and the activity of the streptavidin-biotin method was determined from a single reactor.

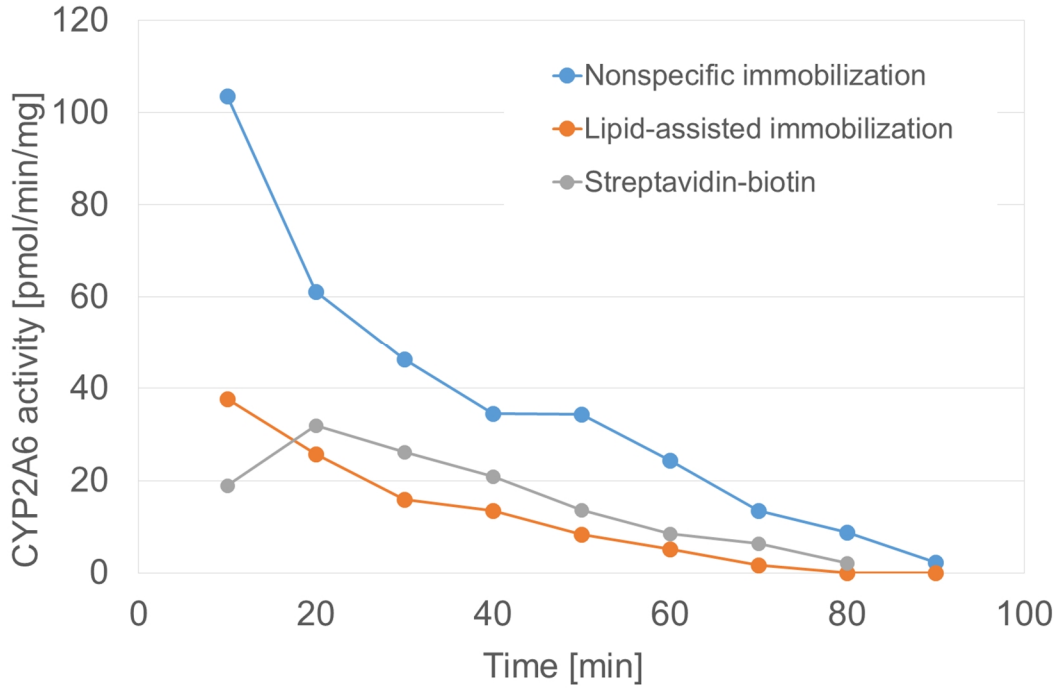

Figure 31. The loss of enzyme activity (as per coumarin 7-hydroxylation *via* CYP2A6 isoenzyme) as a function of time for CYP-IMERs with different immobilization approaches. To measure the activity, 50 µL fractions of the reaction solution were collected with a flow rate of 5 µL/min. n=1 reactor per immobilization approach.

As reaction temperature can affect CYP activity and even the enzyme kinetic parameters (Zaijan *et al.* 2012), stable heating is of paramount importance when performing *in vitro* metabolic studies. Thus, an infrared (IR) camera (FLIR, Wilsonville, OR, USA) was used to confirm uniform heating of the chip at varying flow rates. The IR thermographs of the heated chip with flow rates of 0.5 and 20 µL/min are shown in Figure 32. The chip surface is evenly heated, with the increased flow rate having no apparent effect on the temperature. The small fluctuations of the chip surface temperature are probably due to reflections of IR radiation from the uneven surface of the chip.

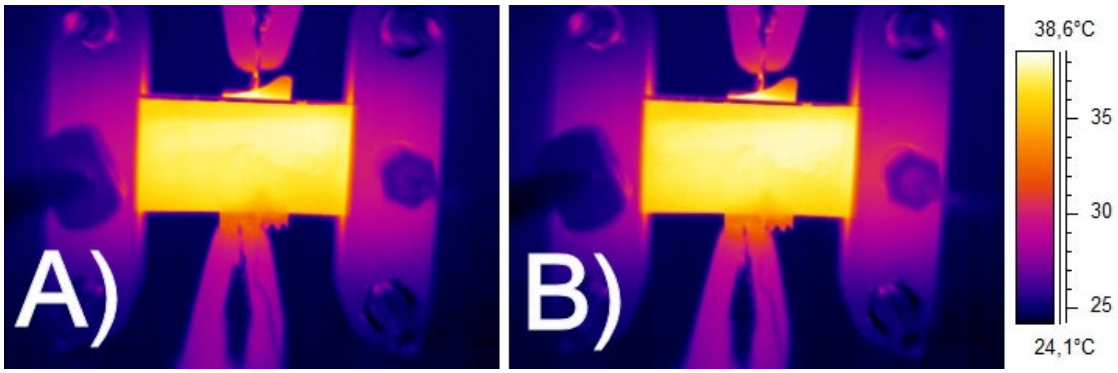

Figure 32. IR thermographs of a thiol-ene pillar chip illustrating the local heating of the chip surface when heated with a resistive heater (R = 0.5 Ω, heating power 0.6 - 0.8 W). A) flow rate 0.5 µL/min B) flow rate 20 µL/min.

5 Discussion

5.1 HLM fusion with fusogenic liposomes

On the basis of literature search, a novel immobilization approach utilizing biotin-labelled fusogenic liposomes was developed. According to Csiszár *et al.* (2010) liposome fusion should not affect cell behavior, which makes it an ideal approach for immobilization of cell-like human liver microsomes. Hypothetically, by utilizing fusogenic liposomes, the strong bonding energies of conventional covalent immobilization can be achieved without its downside of affecting the enzyme activity. The actual immobilization chemistry is based on the strong, specific bonding of biotin and avidin. Avidin is a protein that specifically binds biotin via an extremely strong non-covalent bond. The dissociation constant of the biotin-avidin bond is measured to be $K_D \approx 10^{-15}$ M, making it one of the strongest known non-covalent bonds (Green 1975).

The lipid composition of the FLs was tailored based on literature (Hersch *et al.* 2015) to favor spontaneous fusion with biological membranes. 1,2-dioleoyl-sn-glycero-3-phophoethanolamine (DOPE) is a neutral lipid with a net negative curvature promoting fusion intermediate states. 1,2-dioleoyl-3-trimethylammonium-propane (DOTAP) has a positive charge in the polar headgroup that interacts with the negatively charged cell membrane decreasing the distance between the two membranes consequently increasing the probability of fusion. The polarization of the delocalized π-electrons in the rhodamine moieties is hypothesized to induce membrane instabilities and disorders (Csiszár *et al.* 2010). According to Cevc & Richardsen (1999) such effects could promote membrane fusion.

The size reduction of the fusogenic liposomes after extrusion was monitored both by dynamic light scattering and fluorescence microscopy. The resulting size distribution was somewhat contradictory to expectations, as a size distribution in the range of 100 nm should be expected with the used membrane (Walde & Ichikawa 2001). The manufacturer was also contacted but could not give any clear explanation as to the reason for the unexpected size distribution of the liposomes. One possible explanation is that the membrane is damaged during

the extrusion as a result of excessive backpressure. To prevent this, it is sometimes advisable to extrude the liposome vesicles through multiple membranes with incrementally decreasing pore size (Walde & Ichikawa 2001).

Size distribution of the microsomal vesicles in the HLM solution was also examined using dynamic light scattering. In DLS, vesicle sizes are determined by measuring the scattering of light passing through a sample. The intensity of the scattered light can be calculated from the Rayleigh law (Equation 3):

$$I = I_0 \frac{1+\cos^2\theta}{2R^2}\left(\frac{2\pi}{\lambda}\right)^4\left(\frac{n^2-1}{n^2+2}\right)^2\left(\frac{d}{2}\right)^6 \quad (3)$$

where R is the distance to the particle, d is the particle diameter, n is the refractive index of the particle material and θ is the scattering angle. As the scattering intensity is proportional to the 6th power of the particle diameter, scattering from large particles easily suppresses signals coming from smaller particles in the sample (Li *et al.* 2011). Taking this into account, the contribution of the smallest size fraction in the range of 100-200 nm to the total size distribution is much more prominent than what can be directly inferred from the data.

On the microscopic images taken after the fusion of FLs with HLM, the enrichment of the fluorescence signal on the HLM membrane can clearly be seen. On the basis of the pictures, the fluorescence signal seems to be concentrated on the larger microsomal vesicles. This is likely to hamper the efficiency of HLM biotinylation, as according to the DLS data, the larger microsomal vesicles comprise only a small fraction of the whole vesicle population. This means that a substantial part of CYP activity resides in the small vesicles with a diameter in the range of 100-200 nm.

It is not totally clear whether the FLs of the size used in this study can in fact fuse with the smallest microsomal vesicles. It could be argued that the interaction of two vesicle systems of the same size does not provide sufficient contact area for membrane fusion. In literature, FLs have been used extensively on whole cells (Hersch *et al.* 2015; Naumovska *et al.* 2014; Kleusch *et al.* 2012), in which case, the membrane to be functionalized is considerably larger than the fusogenic

liposome. No research papers on liposome fusion with subcellular fractions could be found. To improve fusion efficacy, the effect of decreasing the size of the liposomes further should be studied. This could be done by extruding through smaller membranes or by using sonication instead of extrusion.

To the best of my knowledge, FLs have not been utilized in HLM functionalization prior to this thesis. The use of FLs in HLM functionalization offers a flexible method for immobilizing microsomal CYP enzymes exploiting different immobilization chemistries. As recombinant-CYP-containing supersomes do not significantly differ from HLMs in terms of biological structure, the technologies developed in this thesis can in principle be easily extended to recombinant CYP models as well.

5.2 HLM immobilization on magnetic particles

The use of streptavidin-coated magnetic beads in immobilizing HLM has been previously described by Kampe *et al.* (2014). The researchers immobilized HLM on the magnetic beads *via* a nonspecific mechanism that was not discussed in detail. This nonspecific binding was taken as a starting point in this thesis and used to roughly optimize the immobilization conditions and to act as a reference to the techniques based on biotin-avidin chemistry.

The nonspecific method constituted a facile and fast method of immobilizing HLM, but the low immobilization yields limit its utilization on analytical applications. In the study by Kampe *et al.* (2014) 3.15 mg of beads were used per one reactor to allow sufficient enzyme activities (cf. 0.25 mg per reaction used in this thesis). The excess consumption of beads compromises the cost-effectiveness of the method, especially if the beads must be frequently replaced due to enzyme inactivation.

By using the novel immobilization method comprising biotin-containing fusogenic liposomes, the enzyme activity of the beads could be increased 3-fold compared to the nonspecific immobilization. By increasing the efficiency of liposome-HLM fusion by the means discussed in the previous chapter, activity could be further improved. Increasing the bead specific activity means that smaller amounts of

beads can be used for generating the same amount of metabolites, which will alleviate the design of microfluidic applications.

The enzyme stability with repeated enzyme incubation cycles remains an issue even with the new immobilization method. According to the results, the immobilized HLM can be stored at 4 °C for extended periods without significant activity loss. Based on this observation, immobilized beads could potentially be prepared in large batches, stored in the refrigerator and used on demand, which facilitates their use. With repeated incubation cycles, activity of the beads drops radically. Thermal inactivation is likely one of the reasons for the loss of enzyme activity. However, according to the preliminary studies conducted on soluble HLM, the enzyme could be incubated at 37 °C for up to 80 min without notable loss of activity, which would suggest that other mechanisms play a greater role. The leaching of enzyme was studied qualitatively with the nonspecific method of immobilization. CYP activity was found in all the tested fractions, which indicates enzyme leaching during all the different steps of the protocol. The gradual loss of activity could be thus explained by leaching, as the particles are exposed to repetitive cycles of heating and mixing. The stronger binding of the biotin-labelled microsomes on the particle surface should hypothetically alleviate the leaching, but the data from the stability studies did not support this hypothesis.

Holmberg *et al.* (2005) showed that biotin-labelled DNA could be reversibly dissociated from streptavidin-coated particles using just elevated temperatures. Rapid and complete elution of the bound biotin was achieved at 70 °C in nonionic aqueous solutions, but significant elution occurred even with lower temperatures in the range of the incubation temperature used in this study. The dissociation of biotin from streptavidin caused by the elevated temperature might partly explain the observed loss of activity. However, the investigators also reported that the presence of salts, especially divalent salts such as $MgCl_2$ used in the incubation buffer in this study, greatly decreased the release of biotin from streptavidin. Taking this into account, it is likely that other forms of inactivation or leaching play a greater role in the observed loss of enzyme activity.

The K_m values of the immobilized enzyme are in good agreement with the values reported in the literature for the soluble enzyme. This is understandable, as the

enzyme resides on the surface of the magnetic particles, with no apparent diffusional constraints or steric blockage of the enzyme. For example, with enzymes immobilized on monolithic supports, K_m is usually increased, as the diffusion of the substrate to the active site is limited (Vlakh *et al.* 2013). The unaffected K_m allows the direct comparison of kinetic studies performed with the immobilized HLM to the results obtained with soluble HLM, which is imperative if this method is to be used in analytical applications. V_{max} was calculated based on the immobilization yield (calculated based on lissamine rhodamine B fluorescence) to be approximately 25% of that of the soluble enzyme. One example was found in the literature, where the effect of immobilization on microsomal enzyme activity was studied (Fernandez-Salquero *et al.* 1993). In the study, the V_{max} was also about 25% of that observed for the soluble enzyme.

The packing of magnetic particles in microfluidic channels proved difficult. Packing the particles too firmly resulted in the generation of backpressure and consequent ejection of the particles from the channel. On another magnet configuration, the particles could be retained in the channel with flow rates of up to 3 µL/min. However, the particles could not be evenly packed inside the reactor. The particles tended to form meandering patterns, concentrating on the channel sides, probably due to lower flow rates in the boundary layer. The uneven packing was confirmed by confocal microscopy imaging. The difficulties in uniform particle packing could lead to reproducibility issues in final applications. The efficiency of the reactor is also compromised, as the whole enzyme capacity is not fully utilized due to inhomogeneous perfusion through the particle mass.

As a solution to the problems in particle packing, a new reactor design (Figure 33) was sketched with AutoCAD® design software according to a design introduced by Tabnaoui *et al.* (2012). The design comprises a magnetically-driven fluidized bed reactor, where the magnetic particles are confined in a steady-state between a magnetic force generated by an external magnet and the hydrodynamic drag forces of the liquid. The fluidized bed design should overcome the limitations of the conventional plug-type reactor, namely the uneven packing and high backpressure. Due to time limitations, the design could not be tested out in practice.

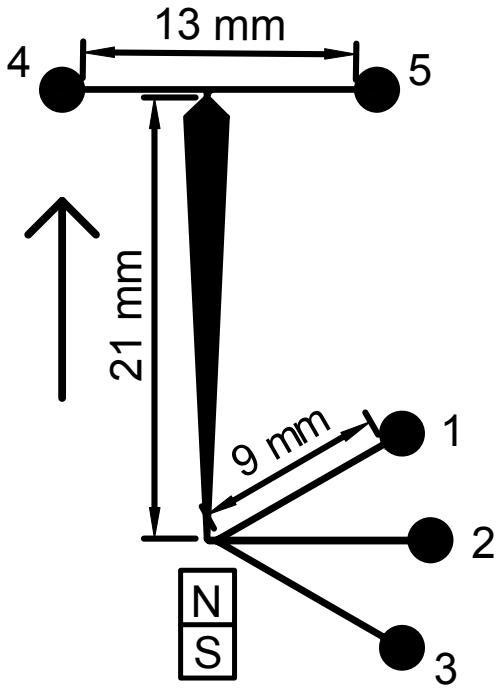

Figure 33. A schematic drawing of the fluidized bed reactor design. 1-3: inlets for e.g. substrate, cosubstrate and inhibitor solutions, 4: inlet for acid, 5: outlet for detection. The direction of flow is denoted by an arrow.

As the uniform packing of magnetic particles inside microfluidic channels is considerably challenging, the direct immobilization of HLM on the functionalized reactor surface might offer a more feasible and straightforward way to preparing CYP-IMERs. However, the use of magnetic particles also has its strengths. For example, IMERs based on direct immobilization have to be disposed of after the enzyme activity has declined, as the immobilized enzyme cannot be renewed. On the contrary, in IMERs comprising magnetic particles, the enzyme content of the can be readily exchanged and particles functionalized with different CYP isoforms can be used in the same channel. On the other hand, when using relatively inexpensive polymers such as thiol-enes in the microchip fabrication process, the disposable nature of the IMERs might not be a significant problem.

Magnetic particles immobilized with HLM could also be readily utilized in digital microfluidics (DMF). In digital microfluidics, discrete droplets are manipulated by controlling the hydrophilicity of a dielectric surface by the application electrical fields (Kirby 2010). With this technology, the droplets can be easily transported, mixed, reacted and analyzed in a highly automated manner. The manipulation of magnetic particles on DMF platforms has been already demonstrated (Choi *et al.*

2013). The use of DMF would allow easy implementation of several parallel metabolic reactions simultaneously with excellent reproducibility. In DMF applications, the cumbersome packing stage the particles is also bypassed.

5.3 CYP-IMERs

Three different immobilization approaches were studied for immobilizing HLM on in-house fabricated thiol-ene chips. The monomer composition of the thiol-ene chip allowed for facile tuning of the surface chemistry for functionalization by manipulating the ratio of thiol and allyl monomers.

The immobilization yields of different methods were compared by determining the enzyme activity of washing fractions collected from the reactor after immobilization and using this data to calculate the amount of enzyme remaining in the reactor. The specific enzyme activity of the eluted fractions was assumed to be the same as the control activity. This assumption likely generated some error to the results, as some activity is presumably lost during the washing process. However, because all the reactors were handled identically, the method allowed the qualitative comparison of the different methods in terms of immobilization efficiency.

The highest initial activity was achieved by binding HLM nonspecifically on the thiol-ene surface (50% allyl excess). A thiol-ene surface with a 50% excess of allyl groups is relatively hydrophilic, with a water contact angle of approximately 75 degrees (Tähkä *et al.* 2015). This probably facilitates interactions with the polar ends of the phospholipids on the microsomes and leads to relatively effective adsorption of the microsomes on the thiol-ene surface. The interaction of phospholipid bilayers with hydrophilic substrates, such as glass, is used routinely in preparing lipid bilayer-coated surfaces (Rädler *et al.* 1995; Yang *et al.* 2001). However, the activity of nonspecifically bound HLM also drops dramatically over time. The rate of decrease in activity is greater compared to the other two tested immobilization methods. This is likely due to greater leaching, as HLM is bound to the reactor surface only by weak interactions. Despite the high initial activity, the nonspecific immobilization method is not likely to be feasible in future applications owing to the rapid drop in activity.

Although the initial activity of the HLM immobilized on the lipid bilayer is considerably lower compared to the nonspecific immobilization method, the decrease in enzyme activity over time seems to be somewhat hampered. It should be noted that because the lipid coating of the reactors was not monitored in any way, the presence of a lipid bilayer cannot be verified with certainty. On the other hand, based on the differences in initial activities and enzyme stability between functionalized and non-functionalized reactors, some difference in the surface chemistries of the two reactors is to be presumed. The phase transition temperature T_m for the thiol-containing lipid used in this study is approximately 60 °C (Anon. 2016b). The immobilization of HLM and the reaction were carried out at temperatures well under T_m, which undoubtedly affected HLM solubilization into the lipid membrane. As temperatures over 60 °C cannot be used due to HLM inactivation, alternative solutions for lipid functionalization of the reactors should be studied in the future.

As the biotin-streptavidin method of immobilization could only be tested once due to time limitations, no definite conclusions can be made. However, it seemed that the decrease in enzyme activity with time could be slowed down by this approach also. Additionally, the fraction of immobilized enzyme was increased with this immobilization method. However, enzyme activity of the reactor was not increased in the same proportion. Further studies are needed to assess the feasibility of this approach for CYP-IMER preparation.

Thermal inactivation likely played a role in the decrease of enzyme activity, as the activity of all reactors faded within 2 hours. The temperature of the reactors was controlled manually by adjusting the output voltage of the voltage supply according to the measured temperature on the reactor surface. The manual control may have led to temporary overheating of the reactor. To level the possible temperature fluctuations, the voltage supply could be attached to a proportional-integral-derivative (PID) controller in the future. Due to the minute reactor volumes, heating power is not an issue with microreactors. The IR thermographs shown in Figure 32 support this, as the channel is uniformly heated even with excessive flow rates. To assess the proportional relevance of enzyme leaching and thermal inactivation, the enzyme activity of the outflowing solution could be determined. The shelf life of the reactors after immobilization was not

studied, but based on the initial experiments on HLM stability, CYP-IMERs could also be prepared in larger batches and stored in the refrigerator for future use, as was envisioned for the magnetic particles. This would greatly facilitate their use, as parallel chips can be easily prepared simultaneously.

Flow rate of the reaction solution affected the reactor activity. As the flow rate was increased, the activity of the reactor started to drop. At 25 µL/min, almost no umbelliferone was detected. Gradual inactivation of the enzyme arguably contributed to the differences in activities observed with different flow rates. However, the increase in activity after restoring the flow rate to 5 µL/min indicates that metabolite production is hampered by high flow rates. This is at least partly explained by the laminar nature of fluid flow in microfluidic environments. In laminar conditions, mixing occurs by diffusion alone, which may result in exceedingly long mixing times (Squires & Quake 2005). As a result, the reaction kinetics of the reactor were presumably limited by diffusion, which sets strict requirements on fluid residence time.

Future work should concentrate on increasing enzyme stability over time by optimizing the immobilization protocols and enhancing temperature control. Possible applications of the CYP-IMER could include drug-drug interaction screening and *in situ* metabolite production for analytical standards. For the use in *in vitro* metabolic studies, the kinetic characteristics of the immobilized HLM should be carefully assessed to ensure correspondence with soluble enzyme assays. In the case of metabolite production, metabolite yields should be optimized.

5.4 Future prospects

Currently, high-performance liquid chromatography (HPLC) is unquestionably the gold standard of pharmaceutical analysis (Görög 2007). The popularity of HPLC is easily understood as it offers a robust and relatively fast means of analyzing complex samples, especially when coupled to a mass spectrometer. However, there are several drawbacks in the traditional analytical methods that are slowing down drug development. A standard HPLC instrument generates over 1 liter of chemical waste on a daily basis (Welch *et al.* 2010). The throughput capacity of

LC-based analysis systems is limited by the fact that increasing sample throughput simultaneously decreases the coverage of detected compounds due to e.g. incomplete resolution of the analytes (de Raad *et al.* 2016). Presently, a typical CYP inhibition assay is performed on a well plate and includes many steps of manual pipetting (Wang & Bell 2012), which greatly limits the throughput of the analysis and generates potential error in the final results.

A drawback of microfluidic systems has been the difficulty of coupling the devices to macro-scale devices such as detectors. This has limited the detection methods that can be used within microfluidic frameworks. Mostly optical detection methods, such as fluorescence detection have been used, which limits the universality of the systems (Wang et al. 2015). Recently, there have been several promising reports of on-line microfluidic-MS analyses (Petersen *et al.* 2012; Gao *et al.* 2012; Nordman *et al.* 2011). Coupling microfluidic systems to MS offers a method of universal and highly sensitive analyte detection, and is very likely to become more common in the future.

With the inherent advantages of microfluidic technology and the recent technological advantages such as facile coupling of microfluidic systems to MS, one could envision a highly parallel microfluidic system for metabolic studies that in addition to a CYP microreactor includes a separation channel and an on-line interface to a mass spectrometer. By using tubing to introduce reagents to the reactor, the amount of manual pipetting could be reduced, increasing analysis accuracy. The use of multiple fluid inlets would also enable the generation of concentration gradients by adjusting flow rates. Combined with on-line detection, this would allow rapid determination of enzyme kinetic parameters. Coupling the reactor to MS would offer a nearly universal approach for detection, with no need for separate, potentially expensive, fluorescent or luminescent probes. With these potential advantages, it is not hard to see microfluidic platforms eventually replacing conventional HPLC assays. If the microreactors developed in this thesis are to be used in *in situ* metabolite production, the ease of integrating different unit operations together in microfluidic devices would allow the reactor to be coupled to e.g. a miniaturized solid phase extraction (SPE) column for facile isolation of the analytes.

One prominent trend in microfluidic metabolic studies is the development of more intricate systems mimicking the *in vivo* conditions with high fidelity. In the so-called organs-on-chips approach, physiological features of tissues and organs are modelled in continuously perfused, micrometer-sized devices. As aspects such as tissue-tissue interfaces and fluid shear stress, which greatly influence organ function, can easily be implemented on microfluidic organ models, they offer a superior model of living tissues when compared to the conventional 2D cell models. Organs-on-chips models can also be linked together to build complex models for studying e.g. drug distribution *in vitro* (Bhatia & Ingber 2014). Even comprehensive human-on-a-chip systems comprising several interlinking microfluidic organ models have been envisioned (van Noort *et al.* 2014) However, it should be noted that there is a trade-off between *in vivo* resemblance and throughput/cost-effectiveness. Even if increasingly complex models are being developed, there is still a demand for systems with lesser *in vivo* resemblance, such as the microreactors studied in this thesis, because of their capability for high-throughput analysis. This is especially true for the early stages of drug development, where thousands of drug candidates have to be screened at the same time and the assays are typically of routine nature, e.g. basic inhibition assays (Materne *et al.* 2015).

Microfluidics has characteristically been a highly technology-driven area of research. Despite its virtually limitless technological possibilities, it has not yet penetrated into the mainstream market. In the pharmaceutical industry, one obstacle in the adaptation of microfluidic technologies are the strict regulatory requirements on method validation, which hamper the adoption of novel technologies (Görög 2007). Additionally, as the microfluidic research still has a very strong academic emphasis, researchers are not often interested in studying e.g. chip-to-chip or batch-to-batch variability, which on the other hand is of utmost importance to the pharmaceutical analysis applications (Volpatti & Yetisen 2014). As the capabilities of microfluidics are more fully realized, the interest of the industry will likely shift the focus of research towards implementation.

6 Conclusions

The aim of this work was to develop novel approaches for creating immobilized enzyme microreactors for studying human drug metabolism on microfluidic platforms. Two main approaches were studied: The immobilization of HLM on commercial streptavidin-coated magnetic particles and the immobilization of HLM on in-house fabricated thiol-ene-based microchips comprising micropillars. As a result, a novel immobilization approach was developed. The developed method was based on biotinylation of HLM with biotin-containing fusogenic liposomes.

With the magnetic particle approach, the use of fusogenic liposomes conferred a 3-fold increase in enzyme activity compared to a previously published method based on nonspecific adsorption. The enzyme kinetic parameters of the immobilized enzyme were comparable to the parameters of soluble HLM obtained from the literature, which is essential for prospective applications in metabolic screening. Enzyme stability remains an issue, as enzymatic activity rapidly decreased with repetitive incubations, likely due to both enzyme leaching and thermal inactivation.

Three different immobilization methods were tested for immobilizing HLM on in-house fabricated thiol-ene microchips. HLM were solubilized on a chip surface functionalized with lipid bilayers and HLM labeled with biotin using fusogenic liposomes was bound on streptavidin-functionalized chip surface. As a control, HLM was also nonspecifically bound on chip surface by physical adsorption. The highest initial activities could be achieved with the nonspecific immobilization method, likely due to the hydrophilic nature of the thiol-ene surface, which facilitates interactions with the polar ends of the lipid bilayers of HLM. With the other two methods, the initial reactor activities were lower, but the gradual decline of enzyme activity could be slowed down, probably due to stronger interactions between the chip surface and HLM. However, the enzyme activity of all the different types of reactors faded within 2 hours. In the future, enzyme stability should be enhanced *via* improved temperature control of the reactor and optimizing the developed immobilization protocols.

In the future, practical applications utilizing the developed immobilization approaches could be developed for *in vitro* studies of human drug metabolism. The use of magnetic particles could be easily implemented on digital microfluidic platforms, or the particles could also be packed inside microfluidic channels comprising magnetic fluidized bed microreactors envisaged in this thesis. For analytical applications, more intricate microfluidic systems comprising separation and on-line MS-detection could be implemented. The thiol-ene microreactors could also be used in metabolic screening. Another valid application for these reactors is the *in situ* preparation of analytical standards of CYP metabolites by optimizing the product yield of the reactors.

7 Acknowledgements

This work was carried out at the Division of Pharmaceutical Chemistry and Technology, Faculty of Pharmacy, University of Helsinki as part of the CUMTAS project (Customized Micro Total Analysis Systems to Study Human Phase I Metabolism, http://cordis.europa.eu/project/rcn/106984_en.html) funded by the European Research Council (grant no. 311705). Confocal microscopy imaging was performed at the Light Microscopy Unit, Institute of Biotechnology. Dr. Ville Jokinen is acknowledged for fabricating the SU-8 masters for the microfluidic chips.

8 References

Akbarzadeh, A., Rezaei-Sadabady, R., Davaran, S., Joo, S.W., Zarghami, N., Hanifehpour, Y., Samiei, M., Kouhi, M. and Nejati-Koshki, K., Liposome: classification, preparation, and applications, *Nanoscale Res. Lett.* **8** (2013) 102.

Anonymous, Frequently asked questions (11205 D), https://www.thermofisher.com/search/results?query=11205D&persona=DocSupport&type=Product+FAQs, 17.7.2016.

Anonymous, Phase transition temperatures for glycerophospholipids, http://avantilipids.com/tech-support/physical-properties/phase-transition-temps/, 30.5.2016.

Bailey, A.L. and Cullis, P.R., Membrane fusion with cationic liposomes: effects of target membrane lipid composition, *Biochemistry* **36** (1997) 1628-1634.

Bajoria, R. and Contractor, S.F., Effect of the size of liposomes on the transfer and uptake of carboxyfluorescein by the perfused human term placenta, *J. Pharm. Pharmacol.* **49** (1997) 675-681.

Batrakova, E.V., Li, S., Vinogradov, S.V., Alakhov, V.Y., Miller, D.W. and Kabanov, A.V., Mechanism of pluronic effect on P-glycoprotein efflux system in blood-brain barrier: contributions of energy depletion and membrane fluidization, *J. Pharmacol. Exp. Ther.* **299** (2001) 483-493.

Becker, H. and Gärtner, C., Polymer microfabrication technologies for microfluidic systems, *Anal. Bioanal. Chem.* **390** (2008) 89-111.

Bhatia, S.N. and Ingber, D.E., Microfluidic organs-on-chips, *Nat Biotech* **32** (2014) 760-772.

Brandon, E.F.A., Raap, C.D., Meijerman, I., Beijnen, J.H. and Schellens, J.H.M., An update on in vitro test methods in human hepatic drug biotransformation research: pros and cons, *Toxicol. Appl. Pharmacol.* **189** (2003) 233-246.

Cabral, J.M.S., Kennedy J.F., Immobilisation techniques for altering thermal stability of enzymes in *Thermostability of enzymes*, ed. Gupta M.N., Springer Verlag, Berlin 1993 pp.163-179.

Celiz, M.D., Tso, J. and Aga, D.S., Pharmaceutical metabolites in the environment: Analytical challenges and ecological risks, *Environ. Toxicol. Chem.* **28** (2009) 2473-2484.

Cevc, G. and Richardsen, H., Lipid vesicles and membrane fusion, *Adv. Drug Deliv. Rev.* **38** (1999) 207-232.

Chernomordik, L.V. and Kozlov, M.M., Mechanics of membrane fusion, *Nat. Struct. Mol. Biol.* **15** (2008) 675-683.

Chesnoy, S. and Huang, L., Structure and function of lipid-DNA complexes for gene delivery, *Annu. Rev. Biophys. Biomol. Struct.* **29** (2000) 27-47.

Choi, K., Ng, A.H.C., Fobel, R., Chang-Yen, D., Yarnell, L.E., Pearson, E.L., Oleksak, C.M., Fischer, A.T., Luoma, R.P., Robinson, J.M., Audet, J. and Wheeler, A.R., Automated digital microfluidic platform for magnetic-particle-based immunoassays with optimization by design of experiments, *Anal. Chem.* **85** (2013) 9638-9646.

Cohen, C.B., Chin-Dixon, E., Jeong, S. and Nikiforov, T.T., A microchip-based enzyme assay for protein kinase A, *Anal. Biochem.* **273** (1999) 89-97.

Copeland, R.A., Enzymes: a practical introduction to structure, mechanism and data analysis, 2nd edition, John Wiley & Sons, New York 2000, 416 p.

Csiszár, A., Hersch, N., Dieluweit, S., Biehl, R., Merkel, R. and Hoffmann, B., Novel fusogenic liposomes for fluorescent cell labeling and membrane modification, *Bioconjugate Chem.* **21** (2010) 537-543.

Culbertson, C.T., Mickleburgh, T.G., Stewart-James, S., Sellens, K.A. and Pressnall, M., Micro total analysis systems: fundamental advances and biological applications, *Anal. Chem.* **86** (2014) 95-118.

Datta, S., Christena, L.R. and Rajaram, Y.R.S., Enzyme immobilization: an overview on techniques and support materials, *Biotech.* **3** (2012) 1-9.

de Raad, M., Fischer, C.R. and Northen, T.R., High-throughput platforms for metabolomics, *Curr. Opin. Chem. Biol.* **30** (2016) 7-13.

Dittrich, P.S. and Manz, A., Lab-on-a-chip: microfluidics in drug discovery, *Nat. Rev. Drug. Discov.* **5** (2006) 210-218.

Dutta, D., Pulsipher, A., Luo, W., Mak, H. and Yousaf, M.N., Engineering cell surfaces via liposome fusion, *Bioconjugate Chem.* **22** (2011) 2423-2433.

Fasinu, P., J. Bouic, P. and Rosenkranz, B., Liver-based in vitro technologies for drug biotransformation studies - a review, *Curr. Drug Metab.* **13** (2012) 215-224.

Fernandez-Salguero, P., Gutierrez-Merino, C. and Bunch, A.W., Effect of immobilization on the activity of rat hepatic microsomal cytochrome P450 enzymes, *Enzyme Microb. Technol.* **15** (1993) 100-104.

Fink, D.W. and Koehler, W.R., pH Effects on fluorescence of umbelliferone, *Anal. Chem.* **42** (1970) 990-993.

Fowler, S. and Zhang, H., In vitro evaluation of reversible and irreversible cytochrome P450 inhibition: current status on methodologies and their utility for predicting drug-drug interactions, *AAPS J.* **10** (2008) 410-424.

Franssila, S., Introduction to Microfabrication, 2nd edition, John Wiley & Sons, New York 2010, 534 p.

Gannett, P.M., Kabulski, J., Perez, F.A., Liu, Z., Lederman, D., Locuson, C.W., Ayscue, R.R., Thomsen, N.M. and Tracy, T.S., Preparation, characterization, and substrate metabolism of gold-immobilized cytochrome P450 2C9, *J. Am. Chem. Soc.* **128** (2006) 8374-8375.

Gao, D., Li, H., Wang, N. and Lin, J., Evaluation of the absorption of methotrexate on cells and its cytotoxicity assay by using an integrated microfluidic device coupled to a mass spectrometer, *Anal. Chem.* **84** (2012) 9230-9237.

Green, N.M., Avidin, *Adv. Protein Chem.* **29** (1975) 85-133.

Guengerich, F.P., Cytochromes P450 in *Metabolism of Drugs and Other Xenobiotics*, eds. P. Anzenbacher and U.M. Zanger, Wiley-VCH Verlag GmbH & Co. KgaA, Weinheim 2012, pp. 27-66.

Guengerich, F.P., Cytochrome P450 and chemical toxicology, *Chem. Res. Toxicol.* **21** (2008) 70-83.

Görög, S., The changing face of pharmaceutical analysis, *TrAC, Trends Anal. Chem.* **26** (2007) 12-17.

Hadd, A.G., Raymond, D.E., Halliwell, J.W., Jacobson, S.C. and Ramsey, J.M., Microchip device for performing enzyme assays, *Anal. Chem.* **69** (1997) 3407-3412.

Hersch, N., Wolters, B., Ungvari, Z., Gautam, T., Deshpande, D., Merkel, R., Csiszar, A., Hoffmann, B. and Csiszár, A., Biotin-conjugated fusogenic liposomes for high-quality cell purification, *J. Biomater. Appl.* **30** (2016) 846-856.

Holmberg, A., Blomstergren, A., Nord, O., Lukacs, M., Lundeberg, J. and Uhlén, M., The biotin-streptavidin interaction can be reversibly broken using water at elevated temperatures, *Electrophoresis* **26** (2005) 501-510.

Honiger, J., Balladur, P., Mariani, P., Calmus, Y., Vaubourdolle, M., Delelo, R., Capeau, J. and Nordlinger, B., Permeability and biocompatibility of a new hydrogel used for encapsulation of hepatocytes, *Biomaterials* **16** (1995) 753-759.

Im, S. and Waskell, L., The interaction of microsomal cytochrome P450 2B4 with its redox partners, cytochrome P450 reductase and cytochrome b5, *Arch. Biochem. Biophys.* **507** (2011) 144-153.

Imaoka, S., Imai, Y., Shimada, T. and Funae, Y., Role of phospholipids in reconstituted cytochrome P 450 3A form and mechanism of their activation of catalytic activity, *Biochemistry* **31** (1992) 6063-9069.

Immordino, M.L., Dosio, F. and Cattel, L., Stealth liposomes: review of the basic science, rationale, and clinical applications, existing and potential, *Int. J. Nanomed.* **1** (2006) 297-315.

Jesionowski, T., Zdarta, J. and Krajewska, B., Enzyme immobilization by adsorption: a review, *Adsorption* **20** (2014) 801-821.

Kampe, T., König, A., Schroeder, H., Hengstler, J.G. and Niemeyer, C.M., Modular microfluidic system for emulation of human phase I/phase II metabolism, *Anal. Chem.* **86** (2014) 3068-3074.

Kiiski, I., Tähkä, S., Sathyanarayanan, G., Haapala, M., Jokinen, V. and Sikanen, T., Immobilized cytochrome P450 microreactors with integrated heaters, *Proceedings of The Twentieth International Conference on Miniaturized Systems for Chemistry and Life Sciences (μTAS 2016)*, 9-13 October, 2016.

Kim, D. and Herr, A.E., Protein immobilization techniques for microfluidic assays, *Biomicrofluidics* **7** (2013) 04150-1.

Kirby, B.J., Micro- and nanoscale fluid mechanics, Cambridge University Press, Cambridge, UK 2010, 536 p.

Kleusch, C., Hersch, N., Hoffmann, B., Merkel, R. and CsiszÃ¡r, A., Fluorescent lipids: functional parts of fusogenic liposomes and tools for cell membrane labeling and visualization, *Molecules* **17** (2012) 1055-1073.

Korzekwa, K.R., In Vitro Enzyme Kinetics Applied to Drug-Metabolizing Enzymes in *Drug-Drug Interactions, Second edition*, ed. A.D. Rodrigues, CRC Press, Florida 2008, pp. 31-51.

Kovarik, M.L., Gach, P.C., Ornoff, D.M., Wang, Y., Balowski, J., Farrag, L. and Allbritton, N.L., Micro total analysis systems for cell biology and biochemical assays, *Anal. Chem.* **84** (2012) 516-540.

Kumar, S., Engineering cytochrome P450 biocatalysts for biotechnology, medicine and bioremediation, *Expert Opin. Drug Metab. Toxicol.* **6** (2010) 115-131.

Li, Y., Lubchenko, V. and Vekilov, P.G., The use of dynamic light scattering and Brownian microscopy to characterize protein aggregation, *Rev. Sci. Instrum.* **82** (2011) 053106.

Li, Z., Zhang, W., Lu, X., Li, J., He, B., Jiang, H., Wang, S., Lu, Z., Wang, C. and Cao, J., Reaction temperature alters chorzoxazone metabolism in carp (Cyprinus carpio) hepatic microsomes, *Fish Physiol. Biochem.* **38** (2012) 1225-1231.

Lin, J.H. and Lu, A.Y.H., Inhibition and induction of cytochrome P450 and the clinical implications, *Clin. Pharmacokinet.* **35** (1998) 361-390.

Ma, B., Zhang, G., Qin, J. and Lin, B., Characterization of drug metabolites and cytotoxicity assay simultaneously using an integrated microfluidic device, *Lab Chip* **9** (2009) 232-238.

Malinin, V.S., Frederik, P. and Lentz, B.R., Osmotic and curvature stress affect PEG-induced fusion of lipid vesicles but not mixing of their lipids, *Biophys. J.* **82** (2002) 2090-2100.

Mao, S., Gao, D., Liu, W., Wei, H. and Lin, J., Imitation of drug metabolism in human liver and cytotoxicity assay using a microfluidic device coupled to mass spectrometric detection, *Lab Chip* **12** (2012) 219-226.

Materne, E., Tonevitsky, A.G. and Marx, U., Chip-based liver equivalents for toxicity testing - organotypicalness versus cost-efficient high throughput, *Lab Chip* **13** (2013) 3481-3495.

McGinnity, D.F., Soars, M.G., Urbanowicz, R.A. and Riley, R.J., Evaluation of fresh and cryopreserved hepatocytes as in vitro drug metabolism tools for the prediction of metabolic clearance, *Drug Metab. Dispos.* **32** (2004) 1247-1253.

Ménard, A., Huang, Y., Karam, P., Cosa, G. and Auclair, K., Site-specific fluorescent labeling and oriented immobilization of a triple mutant of CYP3A4 via C64, *Bioconjugate Chem.* **23** (2012) 826-836.

Morigaki, K., Micropatterned model biological membranes composed of polymerized and fluid lipid bilayers, *Biointerphases* **3** (2008) 85-89.

Munro, A.W., Girvan, H.M., Mason, A.E., Dunford, A.J. and McLean, K.J., What makes a P450 tick?, *Trends Biochem. Sci.* **38** (2013) 140-150.

Munro, A.W., Girvan, H.M. and McLean, K.J., Variations on a (t)heme-novel mechanisms, redox partners and catalytic functions in the cytochrome P450 superfamily, *Nat. Prod. Rep.* **24** (2007) 585-609.

Naumovska, E., Ludwanowski, S., Hersch, N., Braun, T., Merkel, R., Hoffmann, B. and Csiszár, A., Plasma membrane functionalization using highly fusogenic immune activator liposomes, *Acta Biomater.* **10** (2014) 1403-1411.

Nebert, D.W., Nelson, D.R., Coon, M.J., Estabrook, R.W., Feyereisen, R., Fujii-Kuriyama, Y., Gonzalez, F.J., Guengerich, F.P., Gunsalus, I.C., Johnson, E.F., Loper, J.C., Sato, R., Waterman, M.R. and Waxman, D.J., The P450 superfamily: update on new sequences, gene mapping, and recommended nomenclature, *DNA Cell Biol.* **10** (1991) 1-14.

Nicoli, R., Bartolini, M., Rudaz, S., Andrisano, V. and Veuthey, J., Development of immobilized enzyme reactors based on human recombinant cytochrome P450 enzymes for phase I drug metabolism studies, *J. Chromatogr. A* **1206** (2008) 2-10.

Nordman, N., Sikanen, T., Moilanen, M., Aura, S., Kotiaho, T., Franssila, S. and Kostiainen, R., Rapid and sensitive drug metabolism studies by SU-8 microchip capillary electrophoresis-electrospray ionization mass spectrometry, *J. Chromatogr. A* **1218** (2011) 739-745.

Paine, M.J.I., Scrutton, N.S., Munro, A.W., Gutierrez, A., Roberts, G. C. K. and Wolf, C. R., Electron transfer partners of cytochrome P450, in *Cytochrome P450: Structure, Mechanism and Biochemistry*, ed. P. R. Ortiz de Montellano, Kluwer Academic/Plenum, New York 2005, pp. 115-148.

Pelkonen, O., Rautio, A., Raunio, H. and Pasanen, M., CYP2A6: a human coumarin 7-hydroxylase, *Toxicology* **144** (2000) 139-147.

Petersen, N.J., Pedersen, J.S., Poulsen, N.N., Jensen, H., Skonberg, C., Hansen, S.H. and Pedersen-Bjergaard, S., On-chip electromembrane extraction for monitoring drug metabolism in real time by electrospray ionization mass spectrometry, *Analyst (Cambridge, U. K.)* **137** (2012) 3321-3327.

Rädler, J., Strey, H. and Sackmann, E., Phenomenology and kinetics of lipid bilayer spreading on hydrophilic surfaces, *Langmuir* **11** (1995) 4539-4548.

Sakai-Kato, K., Kato, M., Homma, H., Toyo'oka, T. and Utsunomiya-Tate, N., Creation of a P450 array toward high-throughput analysis, *Anal. Chem.* **77** (2005) 7080-7083.

Schindelin, J., Arganda-Carreras, I., Frise, E., Kaynig, V., Longair, M., Pietzsch, T., Preibisch, S., Rueden, C., Saalfeld, S., Schmid, B., Tinevez, J., White, D.J., Hartenstein, V., Eliceiri, K., Tomancak, P. and Cardona, A., Fiji: an open-source platform for biological-image analysis, *Nat. Meth.* **9** (2012) 676-682.

Schneider, E. and Clark, D.S., Cytochrome P450 (CYP) enzymes and the development of CYP biosensors, *Biosens. Bioelectron.* **39** (2013) 1-13.

Sheldon, R.A. and van Pelt, S., Enzyme immobilisation in biocatalysis: why, what and how, *Chem. Soc. Rev.* **42** (2013) 6223-6235.

Sheldon, R., Enzyme immobilization: the quest for optimum performance, *Adv. Synth. Catal.* **349** (2007) 1289-1307.

Shimada, T., Yamazaki, H., Mimura, M., Inui, Y. and Guengerich, F.P., Interindividual variations in human liver cytochrome P-450 enzymes involved in the oxidation of drugs, carcinogens and toxic chemicals: studies with liver microsomes of 30 Japanese and 30 Caucasians. *J. Pharmacol. Exp. Ther.* **270** (1994) 414-423.

Sikanen, T.M., Microchip Technology in Metabolomics, in *Chromatographic methods in metabolomics*, ed. T. Hyötyläinen and S. Wiedmer, The Royal Society of Chemistry, Cambridge, UK 2013, pp. 138-182.

Sikanen, T., Zwinger, T., Tuomikoski, S., Franssila, S., Lehtiniemi, R., Fager, C., Kotiaho, T. and Pursula, A., Temperature modeling and measurement of an electrokinetic separation chip, *Microfluid. Nanofluid.* **5** (2008) 479-491.

Smith, P.K., Krohn, R.I., Hermanson, G.T., Mallia, A.K., Gartner, F.H., Provenzano, M.D., Fujimoto, E.K., Goeke, N.M., Olson, B.J. and Klenk, D.C., Measurement of protein using bicinchoninic acid, *Anal. Biochem.* **150** (1985) 76-85.

Squires, T.M. and Quake, S.R., Microfluidics: fluid physics at the nanoliter scale, *Rev. Mod. Phys.* **77** (2005) 977-1026.

Tabnaoui, S., Malaquin, L., Descroix, S. and Viovy, J-L., Integrated microfluidic fluidized bed for sample preconcentration and immunoextraction, *Proceedings of The Sixteenth International Conference on Miniaturized Systems for Chemistry and Life Sciences (μTAS 2012),* eds. T. Fujii, A. Hibara, S. Takeuchi and T. Fukuba, Chemical and Biological Microsystems Society, Okinawa 2012, pp. 1408-1401.

Tähkä, S.M., Bonabi, A., Nordberg, M., Kanerva, M., Jokinen, V.P. and Sikanen, T.M., Thiol-ene microfluidic devices for microchip electrophoresis: Effects of curing conditions and monomer composition on surface properties, *J. Chromatogr. A* **1426** (2015) 233-240.

Tan, C.Y., Hirakawa, H. and Nagamune, T., Supramolecular protein assembly supports immobilization of a cytochrome P450 monooxygenase system as water-insoluble gel, *Sci. Rep.* **5** (2015) 8648.

Tanaka, E., Clinically important pharmacokinetic drug-drug interactions: role of cytochrome P450 enzymes, *J. Clin. Pharm. Ther.* **23** (1998) 403-416.

Tischer, W. and Wedekind, F. Immobilized Enzymes: Methods and Applications, in *Biocatalysis - From Discovery to Application*, eds. W. Fessner, A. Archelas, D.C. Demirjian, R. Furstoss, H. Griengl, K.-E. Jaeger, E. Morís-Varas, R. Öhrlein, M.T. Reetz, J.-L. Reymond, M. Schmidt, S. Servi, P.C. Shah, W. Tischer, F. Wedekind, Springer Berlin Heidelberg, Berlin 1999 pp. 95-126.

van Noort, D., Park, S, and Nguyen, N-T., Towards human on a chip: recent progress and future perspective, *Micro Nanosyst.* **6** (2014) 215-231.

Vilkner, T., Janasek, D. and Manz, A., Micro total analysis systems. Recent Developments, *Anal. Chem.* **76** (2004) 3373-3386.

Vlakh, E.G. and Tennikova, T.B., Flow-through immobilized enzyme reactors based on monoliths: II. Kinetics study and application, *J. Sep. Sci.* **36** (2013) 1149-1167.

Volpatti, L.R. and Yetisen, A.K., Commercialization of microfluidic devices, *Trends Biotechnol.* **32** (2014) 347-350.

Walde, P. and Ichikawa, S., Enzymes inside lipid vesicles: preparation, reactivity and applications, *Biomol. Eng.* **18** (2001) 143-177.

Wang, J. and Bell, L., Technical Challenges and Recent Advances of Implementing Comprehensive ADMET Tools in Drug Discovery, in *ADME-Enabling Technologies in Drug Design and Development*, eds. D. Zhang and S. Surapaneni, John Wiley & Sons, Inc., Hoboken, NJ 2012, pp. 129-159.

Wang, X., Yi, L., Mukhitov, N., Schrell, A.M., Dhumpa, R. and Roper, M.G., Microfluidics-to-mass spectrometry: A review of coupling methods and applications, *J. Chromatogr. A* **1382** (2015) 98-116.

Welch, C.J., Wu, N., Biba, M., Hartman, R., Brkovic, T., Gong, X., Helmy, R., Schafer, W., Cuff, J., Pirzada, Z. and Zhou, L., Greening analytical chromatography, *TrAC, Trends Anal. Chem.* **29** (2010) 667-680.

Williams, J.A., Hyland, R., Jones, B.C., Smith, D.A., Hurst, S., Goosen, T.C., Peterkin, V., Koup, J.R. and Ball, S.E., Drug-drug interactions for UDP-glucuronosyltransferase substrates: a pharmacokinetic explanataion for typically observed low exposure (AUCi/AUC) ratios, *Drug Metab. Dispos.* **32** (2004) 1201-1208.

Wollenberg, L.A., Kabulski, J.L., Powell, M.J., Chen, J., Flora, D.R., Tracy, T.S. and Gannett, P.M., The use of immobilized cytochrome P4502C9 in PMMA-based plug flow bioreactors for the production of drug metabolites, *Appl. Biochem. Biotechnol.* **172** (2013) 1293-1306.

Wong, L.S., Khan, F. and Micklefield, J., Selective covalent protein immobilization: strategies and applications, *Chem. Rev.* **109** (2009) 4025-4053.

Yang, T., Jung, S., Mao, H. and Cremer, P.S., Fabrication of phospholipid bilayer-coated microchannels for on-chip immunoassays, *Anal. Chem.* **73** (2001) 165-169.

Yuan, R., Madani, S., Wei, X., Reynolds, K. and Huang, S., Evaluation of cytochrome P450 probe substrates commonly used by the pharmaceutical industry to study in vitro drug interactions, *Drug Metab. Dispos.* **30** (2002) 1311-1319.

Yun, C., Yim, S., Kim, D. and Ahn, T., Functional expression of human cytochrome P450 enzymes in Escherichia coli, *Curr. Drug Metab.* **7** (2006) 411-429.

Zanger, U.M., Introduction to Drug Metabolism in *Metabolism of Drugs and Other Xenobiotics*, eds. P. Anzenbacher and U.M. Zanger, Wiley-VCH Verlag GmbH & Co. KGaA, Weinheim 2012, pp. 287-300.

Zguris, J.C., Itle, L.J., Hayes, D. and Pishko, M.V., Microreactor microfluidic Systems with human microsomes and hepatocytes for use in metabolite studies, *Biomed. Microdevices* **7** (2005) 117-125.

Table 2. Preferred and acceptable chemical substrates for in vitro experiments* (9/25/2006)

CYP	Substrate Preferred	Km (μM)	Substrate Acceptable	Km (μM)
1A2	phenacetin-O-deethylation	1.7-152	7-ethoxyresorufin-O-deethylation theophylline-N-demethylation caffeine-3-N-demethylation tacrine 1-hydroxylation	0.18-0.21 280-1230 220-1565 2.8, 16
2A6	coumarin-7-hydroxylation nicotine C-oxidation	0.30-2.3 13-162		
2B6	efavirenz hydroxylase bupropion-hydroxylation	17-23 67-168	propofol hydroxylati on S-mephenytoin-N-demethylation	3.7-94 1910
2C8	Taxol 6-hydroxylation	5.4-19	amodiaquine N-deethylation rosiglitazone para-hydroxylation	2.4, 4.3-7.7
2C9	tolbutamide methyl-hydroxylation S-warfarin 7-hydroxylation diclofenac 4'-hydroxylation	67-838 1.5-4.5 3.4-52	flurbiprofen 4'-hydroxylation phenytoin-4-hydroxylation	6-42 11.5-117
2C19	S-mephenytoin 4'-hydroxylation	13-35	omeprazole 5-hydroxylation fluoxetine O-dealkylation	17-26 3.7-104
2D6	(±)-bufuralol 1'-hydroxylation dextromethorphan O-demethylation	9-15 0.44-8.5	debrisoquine 4-hydroxylation	5.6
2E1	chlorzoxazone 6-hydroxylation	39-157	p-nitrophenol 3-hydroxylation lauric acid 11-hydroxylation aniline 4-hydroxylation	3.3 130 6.3-24
3A4/5**	midazolam 1-hydroxylation testosterone 6 b -hydroxylation	1-14 52-94	erythromycin N-demethylation dextromethorphan N-demethylation triazolam 4-hydroxylation terfenadine C-hydroxylation nifedipine oxidation	33 – 88 133-710 234 15 5.1- 47

* Note that this is not an exhaustive list (created May 1, 2006).

** Recommend use of 2 structurally unrelated CYP3A4/5 substrates for evaluation of in vitro CYP3A inhibition. If the drug inhibits at least one CYP3A substrate in vitro, then in vivo evaluation is warranted.

http://www.fda.gov/Drugs/DevelopmentApprovalProcess/DevelopmentResources/DrugInteractionsLabeling/ucm093664.htm